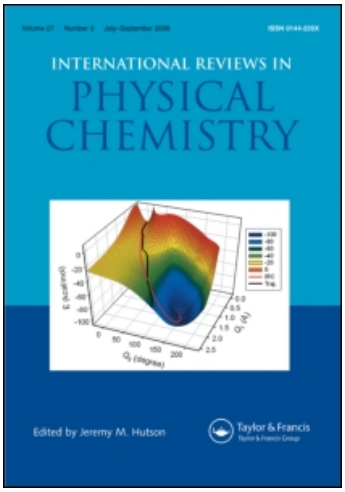

International Reviews in Physical Chemistry
Publication details, including instructions for authors and subscription information:
http://www.informaworld.com/smpp/title~content=t713724383

Rotational line intensities in zero kinetic energy photoelectron spectroscopy (ZEKE-PES)

Frédéric Merkt[ab]; Timothy P. Softley[b]
[a] LCAM, BAT. 351, Universite de Paris XI, Orsay, France [b] Physical Chemistry Laboratory, University of Oxford, Oxford, UK

To cite this Article Merkt, Frédéric and Softley, Timothy P.(1993) 'Rotational line intensities in zero kinetic energy photoelectron spectroscopy (ZEKE-PES)', International Reviews in Physical Chemistry, 12: 2, 205 — 239
To link to this Article: DOI: 10.1080/01442359309353282
URL: http://dx.doi.org/10.1080/01442359309353282

INTERNATIONAL REVIEWS IN PHYSICAL CHEMISTRY, 1993, VOL. 12, NO. 2, 205–239

Rotational line intensities in zero kinetic energy photoelectron spectroscopy (ZEKE-PES)

by FRÉDÉRIC MERKT
LCAM, BAT. 351, Université de Paris XI, 94105 Orsay, France,
and Physical Chemistry Laboratory, University of Oxford,
South Parks Road, Oxford OX1 3QZ, UK

and TIMOTHY P. SOFTLEY
Physical Chemistry Laboratory, University of Oxford,
South Parks Road, Oxford OX1 3QZ, UK

Recent advances in the understanding of the factors which determine line intensities in zero kinetic energy photoelectron spectroscopy (ZEKE-PES) are reviewed. The relative importance of direct ionization and autoionization is assessed. Explicit consideration of the channel interactions which take place in the vicinity of molecular ionization thresholds leads to a general discussion of rotational line intensities in ZEKE-PES. A series of limiting cases is proposed to assist in the interpretation of experimental results. Finally a new dynamical interpretation of ZEKE experiments based on the trapping of the ZEKE electrons in non-penetrating high-l Rydberg orbitals by weak electric fields appears to give a satisfactory explanation of most experimental results obtained to date.

1. Introduction

The aim of the present review is to discuss some recent progress towards a detailed understanding of line intensities in zero kinetic energy (ZEKE) photoelectron spectroscopy. Even though particular attention will be given to rotational line intensities, the principles discussed are general and need to be considered if one wants to extract meaningful information from ZEKE-photoelectron spectra.

Over the last 25 years, photoelectron spectroscopy (PES) (Turner *et al.* 1970, Rabalais 1977, Berkowitz 1979, Eland 1984) has established itself as an extremely useful tool to obtain ionization potentials of atoms and molecules, and the vibronic energy levels of molecular ions. It has also contributed to a better understanding of the photoionization process. PES is an important source of spectroscopic information on ions which, in turn, play a fundamental role in atmospheric physics, plasma physics and interstellar chemistry.

In a PES experiment, one excites molecules above the first ionization threshold with radiation of fixed frequency, and one observes the kinetic energy distribution of the ejected electrons (photoelectrons). PES can be applied without restriction to any neutral molecule that can be formed with sufficient concentration in the gas phase; its only limitation resides in a rather low resolution compared to other spectroscopic methods (typically $80\,cm^{-1}$ and, in some very favourable cases, $20\,cm^{-1}$ (Baltzer 1992)). This is primarily due to the limited resolving power of photoelectron analysers. Despite considerable experimental efforts, it has so far not been possible, using PES, to resolve rotational structure in photoelectron spectra of any molecule apart from H_2 (Åsbrink 1970, Morioka *et al.* 1980, Pollard *et al.* 1982) by single-photon excitation, and

0144-235X/93 $10·00

HBr (Xie and Zare 1989), OH (de Beer *et al.* 1991) and NO at high J values (Wilson 1984, Viswanathan 1986, Allendorf *et al.* 1989, Leahy *et al.* 1991) by resonance-enhanced multiphoton ionization (REMPI).

Another approach to high resolution photoelectron spectroscopy has been the use of tunable light sources combined with geometric and time of flight photoelectron detectors which restrict the detection to 'threshold' photoelectrons (TPE), i.e. photoelectrons with low kinetic energy (Villarejo *et al.* 1967, Baer *et al.* 1969, Spohr *et al.* 1971). Despite a certain improvement in resolution compared with PES, TPES suffers from the presence of unwanted electron signals due to autoionization processes (see for instance Guyon *et al.* (1976), Peatman (1976), Guyon *et al.* (1983), Baer and Guyon (1986)). In the case of H_2, autoionization perturbs the TPE-spectrum to such an extent that the assignment of the rotational structure becomes almost impossible (Peatman 1976).

A more refined way of selecting photoelectrons of low or zero kinetic energy (ZEKE), appropriate for use with pulsed light sources, was proposed and realized experimentally by Müller-Dethlefs, Sander and Schlag (1984a, b). The key idea consists of extracting the photoelectrons at a certain time (0·5–5 μs) after excitation by applying a delayed, pulsed extraction voltage across the ionization region. During the delay time, energetic electrons escape from the ionization region and only ZEKE electrons are detected. As the tunable light source is scanned, peaks in the yield of ZEKE electrons are observed at a series of photoionization thresholds, corresponding to energy differences between the neutral ground state levels and the ionic levels. Using a slight modification of this technique, Reiser *et al.* (1988) could achieve the highest resolution ever observed in a photoelectron spectrum (0·4 cm^{-1}). This pioneering work of Müller-Dethlefs, Schlag and coworkers has opened the way to rotationally resolved photoelectron spectroscopy.

The simplicity of its principle, and the relative ease of its implementation in a spectroscopic experiment have contributed to the large success of ZEKE-photoelectron spectroscopy and its growing number of applications (Grant and White 1991, Müller-Dethlefs and Schlag 1991). These include studies of rotationally resolved angular distribution of the photoelectrons (Reiser *et al.* 1991b) the accurate determination of ionization potentials (see for instance Chewter *et al.* 1987, Reiser *et al.* 1988, Habenicht *et al.* 1991, Harrington and Weisshaar 1992, Kong *et al.* 1992, Wiedmann *et al.* 1992), the investigations of the vibrational structure of large organic molecular ions (Eiden *et al.* 1991, Hillenbrand *et al.* 1991, Ozeki *et al.* 1991a, b, Reiser *et al.* 1991a, Lu *et al.* 1992, Okuyama *et al.* 1992, Rieger *et al.* 1992, Takahashi and Kimura 1992, Takazawa *et al.* 1992), inner-core ionization spectroscopy (Habenicht *et al.* 1990a, b), transition state spectroscopy by ZEKE-photodetachment of negative ions (Waller *et al.* 1990), ZEKE-photodetachment studies of small clusters (Gantefor *et al.* 1990, 1991, Arnold *et al.* 1991, Kistopoulos *et al.* 1991a, b), ZEKE-PES studies of small weakly bound atomic clusters (Harrington and Weisshaar 1990, Tonkyn and White 1991) and molecular clusters (Fischer *et al.* 1992). The technique has also been used recently to study the spectroscopic and dynamical properties of high Rydberg states (Bühler 1990, Haber *et al.* 1991, Bryant *et al.* 1992, Merkt and Softley 1992a, b) and has offered some interesting data for the development of theoretical models describing energy redistribution in highly excited molecular states (Gilbert and Child 1991, Akulin *et al.* 1992, Chupka 1992, Merkt *et al.* 1992a). Finally it has been shown to be a useful tool to probe the vibrational dynamics in aromatic and van der Waals molecules (Zhang *et al.* 1992).

While the power of the ZEKE technique to determine ionization potentials of molecules and ionic rovibronic energies with high accuracy is widely recognized, and has been illustrated in many systems, the interpretation of rotational line intensities still poses some problems: Do the ZEKE line intensities reflect direct ionization cross-sections? Are ZEKE-PES intensities consistent with conventional PES intensities? Can they be predicted by *ab initio* calculations? Are the ionization selection rules, observed in ZEKE-PE spectra, understood? Is there a systematic procedure to extract meaningful information from ZEKE-line intensities?

The beginning of an answer to these questions can be found from the results obtained by TPES, the low resolution precursor of ZEKE-photoelectron spectroscopy. As mentioned above, it is found in most TPES studies that autoionization leads to significant intensity distortions. In fact, the effects of autoionization are so widespread in TPES that they have found an important application in the study of ion–molecule reactions by the TPEPICO method (Baer 1986, 1989, Guyon 1991): owing to autoionization, ions can be prepared in selected vibrational states which cannot be reached by conventional PES because of vanishing Franck–Condon factors. ZEKE-PES would be expected to be less subject to such effects due to its higher resolution and to the fact that the delayed, pulsed extraction method in principle discriminates against fast autoionization while TPES does not. Nevertheless, the question which still arises is to what extent autoionization affects line intensities in ZEKE-spectroscopy.

The purpose of this review article is to address these questions and to summarize the current status of the understanding of photoionization processes as probed by ZEKE-PES. We begin in section 2 with a short review of the different experimental methods which come under the label ZEKE. Section 3 is devoted to assess the importance of direct ionization in ZEKE-PES. In section 4, we focus on the influence of autoionization on ZEKE line intensities and section 5 gives a short survey of what still remains to be understood if one wants to give a full account of line intensities measured in ZEKE-photoelectron spectroscopy.

2. Experimental considerations

The ZEKE experimental set up used by the authors is displayed in figure 2.1 (*a*). Coherent, tunable XUV radiation is generated by sum-frequency mixing the visible or u.v. (frequency doubled or tripled) outputs of two YAG-pumped dye lasers in an atomic free jet of krypton (Fielding *et al.* 1991, Merkt and Softley 1992a, b). The XUV radiation is separated from the unconverted dye laser radiation in a vacuum monochromator. The toroidal geometry of the dispersion grating refocuses the XUV radiation into the photoelectron spectrometer where it is crossed, at its focal point, by a molecular beam of the sample gas. The details of the configuration used to extract the electrons are shown in figure 2.1 (*b*). Two parallel extraction plates with a fine tungsten mesh grid are located on both sides of the ionization region, separated by 1 cm. Pulsed voltages can be applied on both plates independently. The electrons are sent along a 15·5 cm flight tube at the end of which they are detected by an electron multiplier.

ZEKE experiments differ ususally in the source of radiation used for ionization and in subtle variations of the extraction/detection system for the photoelectrons. Some of the currently used systems are briefly reviewed here with their respective advantages.

2.1. *Light sources for ionization*

Whereas discrete frequency sources (for example Helium or Neon lamps) are mostly used in conventional PES, the principles of ZEKE-PES, which rely on the extraction of

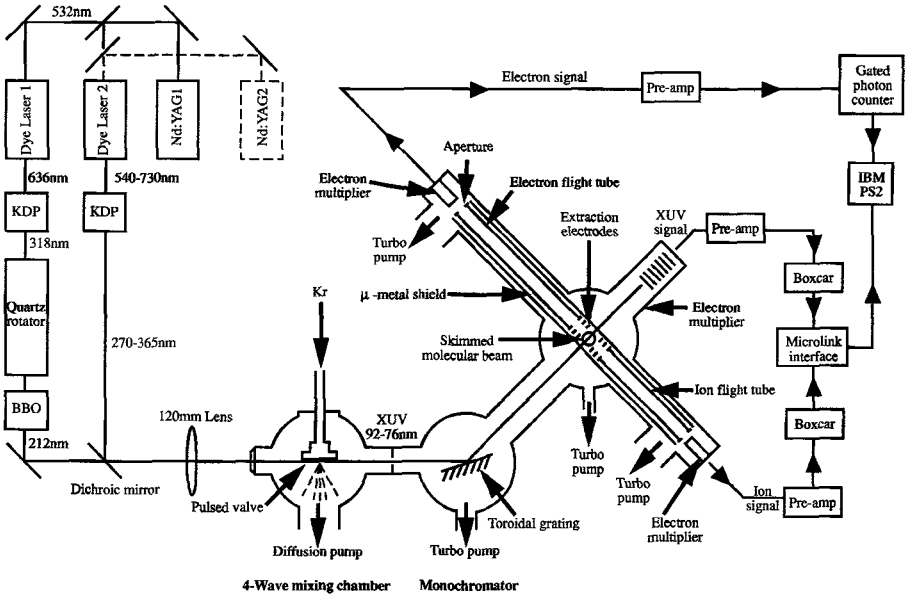

(a)

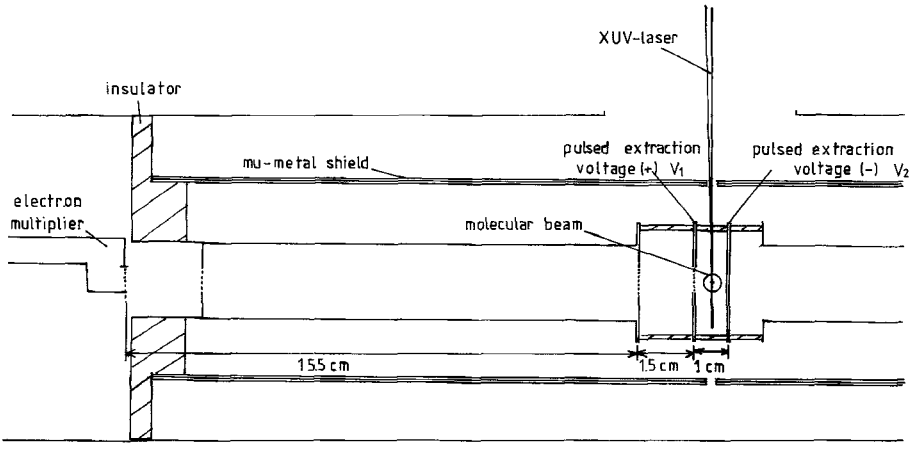

(b)

Figure 2.1. (*a*) Experimental apparatus for XUV generation combined with ZEKE photoelectron and ion extraction. (*b*) Extraction system for the ZEKE photoelectrons.

low (or zero) kinetic energy electrons as a function of the wavelength of the exciting radiation, require the use of tunable light sources, usually tunable lasers. Also, the light source must be pulsed with a pulse duration of approximately 10 ns or less.

The most commonly used method in ZEKE-photoelectron spectroscopy consists of accessing the ionization thresholds by resonance-enhanced multiphoton ionization (REMPI) (see for instance Müller-Dethlefs *et al.* 1984a, Bühler 1990, Haber *et al.* 1991, Takahashi *et al.* 1991, Harrington and Weisshaar 1992) by the use of (1 + 1′) or

(2+1′) excitation schemes. In these experiments, a first laser is used to select a specific excited state of the molecule, and a second laser induces the sequential excitation from the selected intermediate level to the ionization threshold. The selection of an intermediate level in the REMPI process leads to several important advantages: First it is possible, by choosing an intermediate level of appropriate equilibrium geometry, to access a wider range of ionic configurations than by direct ionization. Often, the intermediate states are Rydberg states with low principal quantum numbers, and since these have approximately the same geometry as the ionic state to which they converge, the ionization step is governed by diagonal Franck–Condon factors. Secondly, if sufficient resolution is available to select a single rotational level of the intermediate state, the problem of spectral congestion can be elegantly avoided: Indeed, ionization will only occur to ionic states which can be accessed from the selected intermediate state. Selection rules for ionization from the intermediate level can therefore be obtained experimentally with great clarity. The simplification of the spectra which follows is particularly important in studying ZEKE photoelectron spectra of large organic molecules (Eiden *et al.* 1991, Ozeki *et al.* 1991a, b, Reiser *et al.* 1991b, Lu *et al.* 1992, Okuyama *et al.* 1992) which would otherwise show prohibitively complicated or unresolved structure.

Another approach consists of using VUV and XUV laser systems (for recent review articles on such laser systems, see Stoicheff *et al.* (1985), Vidal (1988), Wallenstein (1988), to reach the ionization thresholds in a direct, one-photon excitation process. Such laser systems are now widely used in spectroscopic experiments. (Recent applications are for instance Ernst *et al.* (1988), Tonkyn and White (1989), Trickl *et al.* (1989), Marangos *et al.* (1990), Merkt and Softley (1990), Fielding and Softley (1991, 1992), Kong *et al.* (1992).) The main advantage of this approach is that it enables a direct comparison with the large bulk of data obtained by conventional photoelectron spectroscopy. As we shall see in section 4, a considerable insight into the factors which lead to ZEKE line intensities can be gained from such a comparison. Another advantage of using one-photon excitation schemes is that the ZEKE-PE spectra consist of rotational progressions which reflect the ground state population and contain, in a compact way, a large amount of information on the ionization process. Finally, one-photon excitation experiments do not require information on intermediate levels—which, in some cases, is not available—and are therefore in principle more universally applicable.

Synchrotron radiation has not yet found application in high resolution ZEKE photoelectron spectroscopy of the valence shells of molecules although some low-resolution pilot studies have been performed (Müller-Dethlefs 1992). The reasons are twofold: first, the monochromators typically used in synchrotron photoionization experiments do not allow for a resolution which is sufficient to make full use of the advantages ZEKE-PES offers compared to TPES. Secondly, the 1 μs delay time between ionization and extraction of the photoelectrons poses difficulties with the high repetition rates of synchrotron cycles (typically 120 ns interval between pulses). It will be shown in the next subsection that this second difficulty can be easily overcome.

Very recently, the use of non-resonant two-photon ionization in ZEKE-PES has been demonstrated (Fischer *et al.* 1992, Strobel *et al.* 1992). Such non-resonant MPI experiments share the advantages of one-photon XUV sources, in that complete rotational progressions can be obtained. The selection rules, however, are different, due to the multiphoton nature of the excitation process (note however the comment made in section 3.3.). In addition, some distortions of the ZEKE profiles could in principle result from accidental near resonances at an intermediate level in the excitation scheme.

2.2. *Photoelectron extraction and detection systems*

The principle of the selection of ZEKE electrons has been outlined in the introduction and is described in detail in a recent review article by Müller-Dethlefs and Schlag (1991) to which the reader is referred for further information.

The first ZEKE spectra were obtained by applying a pulsed extraction electric field approximately 1 μs after ionization (Müller-Dethlefs *et al.* 1984a, b, Sander *et al.* 1987, Habenicht *et al.* 1988). The following behaviour was expected (figure 2.2): electrons which are produced with some velocity component v_y perpendicular to the extraction axis are bound to miss the detector if $v_y t_{tot} > D/2$, where D is the diameter of the electron detector or an aperture placed in front of it, and t_{tot} is the time between ionization and detection. Electrons emitted along the detection axis with some kinetic energy will reach the detector in two bunches, labelled 1 and 3 in figure 2.2(*a*), one bunch corresponding to electrons emitted towards, the other to electrons away from the detector. Discrimination against these two bunches of electrons can be achieved by placing an appropriate detection gate. A judicious positioning of the detection time gate enables the detection of the electrons which are located at the position of ionization when the pulsed extraction field is applied. These electrons, labelled 2 in figure 2.2(*b*) comprise the real ZEKE electrons and, as shown by Reiser *et al.* (1988), those produced by field ionization of long-lived high Rydberg states lying immediately underneath the ionization threshold. In practice, it turns out that, due to small stray electric fields present in the ionization region, the real ZEKE electrons do not contribute to the signal, as they are driven away from the ionization region during the delay time. Therefore recording a ZEKE spectrum by collecting the electrons arriving in a time gate corresponding to 'real' ZEKE electrons (signal 2 in figure 2.2(*b*)) leads to measured ionization thresholds which are slightly red-shifted compared to field-free ionization thresholds.

An important advantage of the delayed pulsed field extraction technique used in ZEKE-spectroscopy is that it allows an efficient discrimination against electrons released by fast autoionization. Such electrons are well known for leading to unwanted signals in threshold photoelectron spectroscopy (Peatman 1976, Baer and Guyon 1986). Figure 2.3(*a*, *b*, *c*) illustrate how this discrimination sets in for the ZEKE

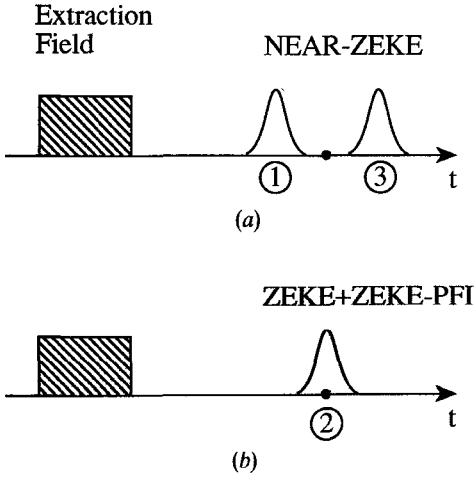

Figure 2.2. Schematic time of flight spectra for (*a*) near ZEKE electrons and (*b*) ZEKE and PFI-ZEKE electrons. See also text.

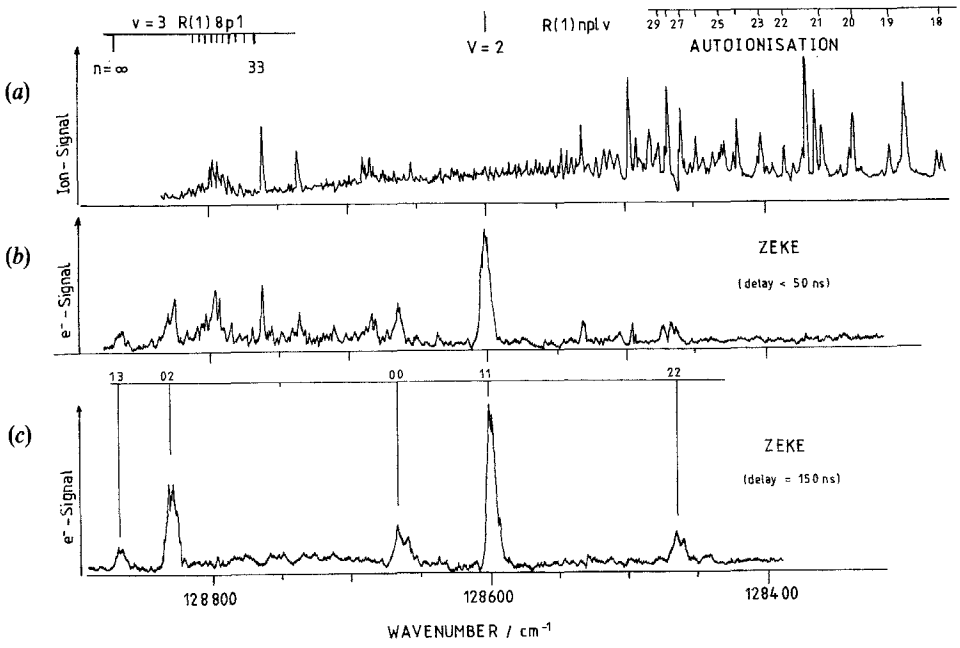

Figure 2.3. Effect of the delay time before the application of the extraction field on the ZEKE spectrum of the $X\,^2\Sigma_g^+(v^+=2)\leftarrow X\,^1\Sigma_g^+(v=0)$ transition of H_2. Delay times (ns): (*a*) 5, (*b*) 50, and (*c*) 150. (From Merkt 1992.)

spectrum of the $X^2\Sigma_g^+(v^+=2)\leftarrow X^1\Sigma_g^+(v=0)$ ionizing transition of H_2. In figure 2.3 (*a*, *b*, *c*) a ZEKE pulsed extraction field of 2 V cm^{-1} is applied 5, 50 and 150 ns after excitation. After 5 ns, the 'ZEKE' spectrum is dominated by autoionization structure. After 50 ns, the Rydberg states on the right of the figure which autoionize to the $v^+=1$ level of H_2^+ (and release electrons with $>2000\,cm^{-1}$ kinetic energy) disappear from the spectrum while the Rydberg states on the left of the figure, which mostly autoionize to the $v^+=2$ level of H_2^+ (and release electrons with $<200\,cm^{-1}$) are still clearly present: The ZEKE structure starts emerging. After 150 ns, the unwanted autoionization structure has been eliminated completely from the ZEKE spectrum. This is in contrast to the TPES spectrum (Peatman 1976) in which fast autoionization cannot be eliminated and dominates the spectrum. Another example of the effect of the delay time on the appearance of a ZEKE spectrum has been shown in the case of N_2 (Merkt and Softley 1992b).

Following the findings of Reiser *et al.* (1988), four slightly different extraction techniques have been developed which all have an important common feature: a delayed pulsed extraction field. Several acronyms have been introduced for these different techniques and a certain confusion has resulted in the literature. Table 2.1 summarizes what the authors refer to when they use the terms ZEKE, or PFI-ZEKE in this article. The various detection methods currently in use are briefly described here.

2.2.1. *The slowly growing pulse technique*

One can estimate the lowering of the ionization threshold caused by an electric field E by using a classical model: assuming a spherically symmetric potential around the

Table 2.1. Different detection techniques used in ZEKE-photoelectron spectroscopy.

Shaped-pulse ZEKE experiment	*near-ZEKE experiment*
One shaped pulsed electric field. Detection of electrons by field ionization (Reiser *et al.* 1988).	One pulsed field. Detection of electrons with low kinetic energy (Reiser *et al.* 1991a).
ZEKE/PFI-ZEKE	
PFI-ZEKE experiment	*MATI experiment*
Two electric fields. Detection of electrons by field ionization (Tonkyn *et al.* 1989) (Haber *et al.* 1991), (Merkt and Softley 1992a).	Two electric fields. Detection of ions by field ionization (Zhu and Johnson 1991).

molecular core, the potential along the z axis experienced by a Rydberg electron in the presence of an electric field is given, in atomic units, by $V(z) = -Ez - 1/z$. The position of the maximum in this one-dimensional surface corresponds to the new ionization threshold and is obtained by solving $dV(z)/dz = 0$, from which the lowering of the threshold is found to be $2\sqrt{E}$ or, more conveniently:

$$\Delta IP/(\text{cm})^{-1} = 6[E/V(\text{cm})^{-1}]^{1/2}. \quad (1)$$

If a slowly growing extraction field is used, the highest Rydberg states are field ionized first. Field ionization of lower Rydberg states occurs, according to equation (1), as the magnitude of the extraction pulse increases. As a result, electrons which correspond to different Rydberg states reach the detector at different times. It is therefore possible to restrict the detection to a particular section of the pseudo-continuum of high Rydberg states below a specific threshold by using a convenient detection time gate. Using this method, Reiser *et al.* (1988) could achieve the highest resolution ($0{\cdot}4\,\text{cm}^{-1}$) ever observed in a photoelectron spectrum.

2.2.2. *The near-ZEKE method*

This method consists of placing a time gate so as to restrict the detection to electrons which have been emitted with a small amount of kinetic energy above a specific ionization threshold. These electrons are called 'near-ZEKE' electrons and are labelled 1 and 3 in figure 2.2 (*a*). The great advantage of this experiment is that it allows a measurement of the angular distribution of the ZEKE photoelectrons. In practice, however, measurements of angular distributions are difficult to realise because the arrival time of the near-ZEKE electrons depends critically on the magnitude and the direction of stray fields, which might change in the course of a measurement. Furthermore, there is always the possibility that some electrons released with some kinetic energy by autoionization contribute to the signal, which complicates the interpretation. A control of these effects is by no means straightforward and requires the greatest care. So far, only one measurement of angular distributions in a ZEKE-PES experiment has been reported (Reiser *et al.* 1991b). Further measurements would be desirable, as angular distributions contain some very important information on the ionization process.

2.2.3 *The pulsed field ionization (PFI) ZEKE method*

Another method of achieving high resolution consists of using two electric fields. The first can be either continuous (Tonkyn *et al.* 1989) or pulsed (Merkt and Softley 1992a) while the second field is pulsed in both cases. The timing of a ZEKE experiment involving two pulsed fields is illustrated in figure 2.4. The first 'discrimination' pulse (E_1) serves the joint purpose of removing from the ionization region all electrons released by direct ionization or by fast autoionization and of field ionizing the Rydberg states lying just below threshold, according to equation (1). Therefore, when the second 'extraction' pulse E_2 is applied, the electrons occupying the highest Rydberg states have already been removed by E_1 and only the lower Rydberg states are field ionized and detected. The resolution expected in a ZEKE experiment involving two pulsed electric fields is given, in first approximation, by equation (2).

$$\Delta\nu/(\text{cm})^{-1} = 6[(E_2(\text{in } V/\text{cm}))^{1/2} - (\text{E}_1(\text{in } V/\text{cm}))^{1/2}]. \tag{2}$$

For instance, a resolution of 0·9 cm^{-1} is predicted for values of 2·5 and 3 $V(\text{cm})^{-1}$ for E_1 and E_2 respectively.

The advantages of the two pulse experiment are the following:

(*a*) The timescale of the experiment can be reduced considerably since the discrimination against energetic electrons is achieved by the discrimination field rather than during the 1 μs waiting time. This is of particular interest in view of using synchrotron radiation in ZEKE experiments. Indeed, the two pulses can easily be applied during the interval of 120 ns between two synchrotron pulses.

(*b*) If the first pulse is applied directly after ionization, it will extract the electrons released by direct ionization or fast autoionization. Therefore, measuring the signal originating from these electrons as as function of the wave-number leads to a spectrum which is similar to a photoionization spectrum recorded by measuring the ion production.

(*c*) Different sections of the pseudo-continuum of high Rydberg states below the ionization threshold can be probed by adjusting the values of E_1 and E_2.

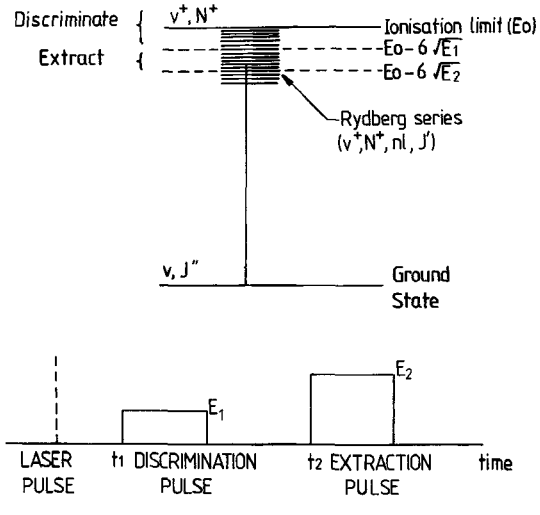

Figure 2.4. Timing and principles of a ZEKE experiment involving two pulsed electric fields.

2.2.4. *The MATI method*

The method is in many ways similar to the PFI-ZEKE method as it also uses two extraction electric fields, but instead of applying the two pulsed fields successively across the same region of space, the two electric fields are applied in distinct regions of space. The sample gas is expanded in a beam of well defined direction. The first electric field is applied in the excitation region and has an effect on the motion of the ions which are produced by fast autoionization or field ionization while it leaves the motion of neutral molecules excited in high Rydberg states unaffected. When these excited neutral molecules enter a second region of space, across which a stronger field is applied, they are field ionized. The motion of the ions produced by the second extraction field is significantly different from that of the ions produced in the excitation region and they can be detected separately. The interest of that technique is that it can be used to record a 'ZEKE' spectrum by collecting the *ions* extracted by the second field E_2 instead of the *electrons*. The method is therefore adapted to record PFI-ZEKE spectra of mass-selected molecules and has been called MATI for mass-analysed threshold ionization. The equivalence of the ion- and electron 'MATI-PFI-ZEKE' spectra of pyrazine has been demonstrated by Zhu and Johnson (1991).

3. Direct ionization in ZEKE-photoelectron spectroscopy

3.1. *General considerations*

It was acknowledged in section 2 that nearly all ZEKE photoelectron experiments involve pulsed-field ionization of very high Rydberg states just below threshold, rather than extraction of true ZEKE electrons at, or above threshold. The Rydberg states form a pseudo-continuum, and as a consequence of the continuity of the transition probability, on either side of an ionization limit, it is generally assumed (as below) that the ZEKE transition intensities can be treated in the same manner as true photoionization intensities.

A common approach to the theoretical analysis of ZEKE rotational line intensities assumes that the final states reached in the excitation process belong to independent ionization channels. In this case, direct ionization cross-sections can be evaluated separately for each ionization channel. Before we proceed and discuss some models based on this assumption, a few comments are necessary. This assumption, which is equivalent to neglecting all interactions between different channels, in particular autoionization, is in general not valid even for conventional photoelectron spectroscopy. Indeed, if the monochromatic excitation frequency corresponds to a transition to a discrete neutral state above the first ionization limit, the cross-section to the ionization continuum can be severely affected by an interaction with this discrete neutral state (Smith 1970a, b, Eland 1984). A particularly striking example of the importance of the excitation frequency (and its coincidence with transition frequencies to discrete neutral states) can be found in the photoelectron spectroscopy of O_2. The HeI (Edqvist *et al.* 1970) and HeII (Baltzer *et al.* 1992) photoelectron spectra of the $X\,^2\Pi_g$–$X\,^3\Sigma_g^-$ transition consist of a short vibrational progression up to $v^+ = 5$, and the transition intensities to the various members of the progression are governed by Franck–Condon factors between molecular and ionic states; the ionization is direct. In contrast, the NeI photoelectron spectrum (Samson and Gardner 1977) of the same transition reveals an extensive progression up to $v^+ = 20$. In the threshold photoelectron (TPE) spectrum (Merkt *et al.* 1992b), the X-state of the ion can even be followed up to $v^+ = 27$. The intensity distortions observed in the NeI spectrum originate from the coincidence between the exciting frequency and a broad resonance seen in the

photoionization spectrum (Guyon and Nenner 1980), while the long progression seen in the TPES is due to the high density of Rydberg states converging to the a and A states of the ion which autoionize towards the almost degenerate high v^+ thresholds of the X state. High v^+ members of the X state are also observed in the ZEKE spectrum (Kong *et al.* 1992).

In conventional photoelectron spectroscopy, it is in principle always possible to choose the excitation frequency so that it does not overlap with any resonance in the absorption/photoionization spectrum (this is especially true if synchrotron radiation is used), and therefore observe, to a good approximation, direct ionization cross-sections. The situation is different in TPES and ZEKE-PES, as these techniques rely on the detection of threshold electrons as a function of the exciting frequency. Since the excitation frequency cannot be chosen, it is impossible to avoid accidental coincidences with transitions to autoionizing Rydberg states although in REMPI experiments it may be possible to change the transition probabilities to the autoionizing state by selection of a different intermediate level. In fact, the number of autoionizing states which lie in the vicinity of a given threshold is often significant: there are series of Rydberg states converging to each higher-lying rovibronic state of the ion. Hence it is likely that at least one of these Rydberg states will accidentally lie within the ZEKE pseudo-continuum of high Rydberg states, and distort the ZEKE line intensities by interactions between different electronic, spin–orbit, vibrational or rotational channels. Above threshold, these interactions would lead to electronic, spin–orbit, vibrational and rotational autoionization respectively. The assumption of non-interacting channels (or direct ionization) is therefore only a coarse (even though often useful, see below) approximation for the evaluation of ZEKE-PES line intensities. Whereas ionization in PES can be treated as a one-channel problem under some conditions, the interpretation of ZEKE-PES intensities is in essence a *multichannel* problem.

Despite the importance of channel interactions for ZEKE line intensities, much of the early one-photon ZEKE work was interpreted in terms of direct ionization, with examples including O_2 (Tonkyn *et al.* 1989), NO_2 (Wiedmann *et al.* 1991) and CO_2 (Fielding *et al.* 1991). In some cases, a reasonable agreement is found, offering support to the assignment of the spectra. In others, however, some anomalies have been noticed: the intensity of the low frequency part of the ZEKE spectrum of several vibrational members of the ground electronic state of NO_2^+ Wiedmann *et al.* 1991) could not be fitted by theoretical expressions for rotational line intensities in direct ionization (Buckingham *et al.* 1970), while a prominent peak in the ZEKE spectrum of CO_2 (Fielding *et al.* 1991) could only be explained by invoking an apparently forbidden transition (Merkt 1992).

Ab initio models for direct ionization have subsequently been applied to simulate ZEKE- and conventional PE spectra of a number of molecules including HBr (Xie and Zare 1989, Lefebvre-Brion 1990a, Wang and McKoy 1991a), O_2 (Braunstein *et al.* 1992), NO (Viswanathan *et al.* 1986, Wang *et al.* 1991), OH and OD (de Beer *et al.* 1991, Wiedmann *et al.* 1992), H_2O (Lee *et al.* 1992a, b, Wiedmann and White 1992) and HCl (Haber *et al.* 1991, Wang and McKoy 1991b). In addition, *ab initio* approaches to ZEKE or PES rotational line intensities have highlighted the importance of shape resonances (Braunstein *et al.* 1992) and Cooper minima (Wang *et al.* 1991) in ZEKE spectroscopy.

The remaining parts of this Section are devoted to a brief discussion of these approaches, leaving the discussion of autoionization effects in ZEKE spectroscopy to Section 4.

3.2. *The model of Buckingham* et al. *(1970)*

The first expressions for rotational line intensities in the PE-spectra of diatomics were derived by Buckingham *et al.* (1970) and Sichel (1970), before Åsbrink (1970) obtained the first rotationally resolved photoelectron spectrum (of H_2) using the NeI discrete source. This pioneering work turned out to be of fundamental importance in the development of theoretical interpretations of rotational line intensities in PE spectroscopy. It has since been extended and refined in three directions: first, it has been reformulated in a more compact form using spherical tensor methods, and has provided the basis for a relatively simple fitting procedure of experimental results as well as a direct physical interpretation of the fitting parameters (Xie and Zare 1992). Secondly, use of the model has led to the derivation of general selection rules in photoionization of diatomic (Xie and Zare 1990) and polyatomic molecules (Müller-Dethlefs 1991). Finally, it has opened the way to sophisticated *ab initio* approaches to rotational line intensities in photoelectron spectroscopy (see section 3.4. below). In view of the large impact of the model of Buckingham *et al.* (1970) on further theoretical developments and of the ease with which it can be used by experimentalists to obtain a rapid fit of their data, some of its essential features are summarized here. The model is based on the evaluation of direct differential ionization cross-section σ_Ω according to the formula:

$$\sigma_\Omega = \frac{8\pi^3 e^2 \nu}{c n_g} \sum_{\text{deg. states}} \left\langle f_k \middle| \sum_i z_i \middle| g \right\rangle^2, \tag{3}$$

where g represents the ground molecular state with statistical weight n_g, which is described by functions of the type $|n''\Lambda''S''J''\Omega''M_J''\rangle$ or $|n''\Lambda''S''N''J''M_J''\rangle$ depending on whether the state obeys Hund's case (*a*) or (*b*) (Herzberg 1989). The final state f is a product of the ionic state ($|n^+\Lambda^+S^+J^+\Omega^+M_J^+\rangle$ or $|n^+\Lambda^+S^+N^+J^+M_J^+\rangle$) and of the free electron wavefunction

$$|k\rangle = \frac{1}{4\pi} \sum_{l=0}^{\infty} \mathrm{i}^l (2l+1) R_l(r) P_l(\mathbf{k}\cdot\mathbf{r}/kr).$$

In these expressions, J, Ω and M_J represent the quantum number of the total angular momentum and its projection on the molecular and space fixed z axis respectively while N, Λ, and S have their usual spectroscopic meaning. The ground state quantum numbers are labelled with superscript " while the ionic states are labelled with a '+'. l corresponds to the orbital angular momentum of the photoelectron, R_l to the radial part of its wavefunction and P_l to a Legendre polynomial.

Ionization is assumed to occur vertically from a definite molecular orbital $u_{n\lambda}$ which is expanded in a single-centre basis set (λ corresponds to the projection of the orbital angular momentum l on the molecular axis).

$$u_{n\lambda} = \sum_{l=\lambda}^{\infty} C_{nl} R_{nl}(r) Y_{l,\lambda}(\theta', \phi'). \tag{4}$$

The centre ($r=0$) of the expansion (4) corresponds to the centre of mass. $R_{nl}(r)$ represents the radial part of the bound orbital and $Y_{l,\lambda}(\theta', \phi')$ a spherical harmonic referenced to the molecular frame. The total cross-section for direct ionization can then be written as a sum of products

$$\sigma_{\text{tot}} = \text{const} \sum_{l=\lambda}^{\infty} \frac{1}{2l+1} Q(l) |C_{nl}|^2 [l|F_{nl}^{E,l-1}|^2 + (l+1)|F_{nl}^{E,l+1}|^2], \tag{5}$$

Table 3.1. Analytical expressions for the Q(l) factors for different Hund's cases.

Case (*b*)←case (*b*):

example: $H_2^+X\ ^2\Sigma_g^+(N^+,\Lambda^+)\leftarrow H_2X\ ^1\Sigma_g^+(J'',\Lambda'')$

$$Q(l)=(2N^+ +1)\begin{pmatrix} N^+ & l & J'' \\ -\Lambda^+ & -\lambda & \Lambda'' \end{pmatrix}^2$$

Case (*a*)←case (*a*):

example: $CO_2^+X^2\Pi_g(J^+,\Omega^+,S^+,\Sigma^+)\leftarrow CO_2X\ ^1\Sigma_g^+(J'',\Omega'',S'',\Sigma'')$

$$Q(l)=(2J^+ +1)(2S''+1)\begin{pmatrix} S^+ & \frac{1}{2} & S'' \\ \Sigma^+ & -\Delta\Sigma & -\Sigma'' \end{pmatrix}^2 \sum_\chi (2\chi+1)\begin{pmatrix} l & \frac{1}{2} & \chi \\ -\lambda & \Delta\Sigma & -\Delta\Omega \end{pmatrix}^2 \begin{pmatrix} J^+ & \chi & J'' \\ -\Omega^+ & \Delta\Omega & \Omega'' \end{pmatrix}^2$$

with $\chi=l\pm\frac{1}{2}$

Case (*b*)←case (*a*):

example: $NO^+X\ ^1\Sigma_g^+(N^+,\Lambda^+,S^+,\Sigma^+)\leftarrow NO\ X^2\Pi(J'',\Omega'',S'',\Sigma'')$

$$Q(l)=(2N^+ +1)\sum_\chi (2\chi+1)\begin{pmatrix} l & S'' & \chi \\ \lambda & \Sigma'' & \Lambda^+ -\Omega'' \end{pmatrix}^2 \begin{pmatrix} N^+ & \chi & J'' \\ -\Lambda^+ & \Lambda^+ -\Omega'' & \Omega'' \end{pmatrix}^2$$

Case (*b*)←case (*b*):

example: $O_2^+X^2\Pi_g(J^+,\Omega^+,S^+,\Sigma^+)\leftarrow O_2X^3\Sigma_g^-(J'',N'',\Lambda'')$

$$Q(l)=\frac{(2J^+ +1)}{(2S^+ +1)}\sum_\chi (2\chi+1)\begin{pmatrix} l & S^+ & \chi \\ -\lambda & \Sigma^+ & \Lambda''-\Omega^+ \end{pmatrix}^2 \begin{pmatrix} J^+ & \chi & N'' \\ -\Omega^+ & \Omega^+ -\Lambda'' & \Lambda'' \end{pmatrix}^2$$

in which $Q(l)$ describes the angular part of the problem (describing mainly the change from molecular to space fixed axes), while the term in square brackets contains a sum of bound-free radial transition integrals $F_{nl}^{E,l'}$. The angular momentum selection rules are determined from the expressions for the $Q(l)$ factors in equation (5) which take different forms depending on the Hund's coupling cases describing the molecular and ionic states. These expressions for the $Q(l)$ are summarized in table 3.1. Experimental PES or ZEKE-PES rotational line intensities should, in principle, be easily fitted to expression (5); the fitting procedure involves calculating numerical values for the $Q(l)$ expressions given in table 3.1 and optimizing the parameter $a_l=|C_{nl}|^2[l|F_{nl}^{E,l-1}|^2+(l+1)|F_{nl}^{E,l+1}|^2]$ in a least squares fit procedure. It can be seen from table 3.1 that the maximum change in core rotational angular momentum observed in direct ionization is determined by the convergence of the expansion (4). In fact, a qualitative description of rotationally resolved photoelectron spectra of diatomic molecules can be obtained easily by considering equation (4): for instance, in the case of the $X\ ^2\Sigma_g^+$–$X\ ^1\Sigma_g^+$ ionizing transition in H_2, where the photoelectron is ejected from the $1s\sigma_g$ molecular orbital, the single centre expansion converges very rapidly, the $l=0$ component being dominant with a weaker contribution from the $l=2$ term (Wilkins and Taylor 1968); thus, the maximum change in core rotation angular momentum should be restricted to ± 2, in agreement with experimental results (Åsbrink 1970, Morioka *et al.* 1980, Pollard *et al.* 1982, Merkt and Softley 1992a). In the π_g^{-1} ionization of O_2, the most significant terms in the expansion (4) correspond to $l=2$ and $l=4$ and therefore a rotationally resolved spectrum is expected to have branches with higher (N^+-J'') values. This is confirmed by experiment (Tonkyn *et al.* 1989). Finally in the ionization out of the C-state of VO, an electron is ejected from the $3d\sigma$ Rydberg orbital centred on the V

atom which is significantly displaced from the centre of mass. The expansion (4), starting with $l=2$, is therefore expected to converge only slowly, leading to very large changes in core rotation, as confirmed by the experimental results of Harrington and Weisshaar (1992). Very recently, the model of Buckingham *et al.* (1970) had been reformulated by Xie and Zare (1992) using the more compact spherical tensor method and extended to take the polarization (alignment, orientation) of the molecular sample into account. In addition, the derived expressions were successfully applied to simulate the (1 + 1) REMPI-PE spectrum of NO measured by Leahy *et al.* (1991) and those lines of the ZEKE-PE spectrum of H_2 which are not perturbed by autoionization (see section 3.4.).

3.3. *Selection rules in direct ionization*

As pointed out above, selection rules for angular momentum changes in photoelectron spectroscopy of diatomics can be derived directly from table 3.1. As an example, we illustrate how this can be done in the particular case of H_2: the $1s\sigma_g$ orbital from which the electron is ejected can be represented almost completely by retaining only the s ($l=0$) and d ($l=2$) terms in expansion (4) (Wilkins and Taylor 1968). Both the $X\ ^1\Sigma_g^+$ state of H_2 and the $X\ ^2\Sigma_g^+$ state of H_2^+ can be represented by Hund's case (*b*) and therefore the first line of table 3.1 has to be used; the 3*j* symbol vanishes unless $N^+ - J'' = 0, \pm 2$. The selection rules which can be derived from table 3.1 are equivalent to those one obtains with the rotation-spectator model (Dixon *et al.* 1971, Duxbury *et al.* 1983) and have been verified in a number of cases. The rotation-spectator model applies well to situations in which the photoelectron escapes rapidly to regions where it only perceives a Coulombic potential. It is interesting to note that within the framework of the rotation-spectator model, ZEKE spectra obtained by one-photon or non-resonant two-photon excitation should be governed by the same selection rules since the electron takes away the angular momentum of the photon(s).

The rotation spectator model is somewhat idealized, as the photoelectron can be 'scattered' by the non-spherically symmetric components of the molecular core potential, an effect leading to l mixing of the outgoing wave (Rudolph *et al.* 1988a, b, Wang *et al.* 1991). In the case of l mixing by the core potential, the selection rules can still be obtained from table 3.1, but by replacing l by a quantum number j (Buckingham *et al.* 1970) which corresponds to the vector addition $l'+1$ of the orbital angular momentum l' of the departing electron (which has experienced l mixing by the potential of the molecular core; note the differences between l and l') and the photon angular momentum. This l mixing of the photoelectron wave by the non-Coulombic terms of the core potential has been proposed to explain the presence of apparently 'forbidden' rotational lines in the ZEKE-photoelectron spectrum of H_2O (Lee *et al.* 1992a, b). An alternative explanation for these lines is based on the effect of bound state–continuum interactions between different channels induced by the dipole of the ion core (Gilbert and Child 1991). The difference between these two interpretations seems rather subtle at first sight, as both invoke the effects of the dipole of the ion core to account for the 'forbidden' lines. There is however an important difference which will become clearer in section 4: the l-mixing interpretation is consistent with a direct ionization approach to ZEKE-rotational line intensities, and, if it predicts a 'forbidden' transition associated with a *negative* change in core rotation angular momentum, it will also predict a 'forbidden' transition associated with a *positive* change (of the same magnitude) in the core rotational angular momentum. The channel-interaction interpretation, on the other hand, relies on an autoionization mechanism to explain the presence of 'forbidden' lines: such a mechanism only becomes operative if an autoionizing Rydberg

state lies within the range of energies probed by the ZEKE-experiment. This results, in general, in a strong difference in the intensity of 'forbidden' lines for negative compared with positive changes in core-rotation (see Section 4 below).

General selection rules for the photoionization of diatomics have been derived by Xie and Zare (1990) for all possible Hund's cases of the initial molecular and final ionic state. These selection rules are consistent with those one can derive from table 3.1 when l is replaced by j as discussed above. They are more complete, as they include Hund's cases (*c*) and (*d*) as well as parity selection rules. The parity selection rules derived by Xie and Zare (1990) generalize and confirm results obtained by Dixit and McKoy (1986) and Raseev and Cherepkov (1990). Hund's case (*e*) has been considered by Lefebvre-Brion (1990b) and Frohlich *et al.* (1991).

Rotational symmetry selection rules for the ionization of polyatomic molecules have been derived by Müller-Dethlefs (1991). The approach used in the derivation of these selection rules is original in that it treats the ionization in the same way as transitions to very high Rydberg states (governed by Hund's case *d*) and is therefore particularly well-suited to ZEKE-photoelectron spectroscopy. These selection rules have been successfully applied to explain the difference between the rotationally resolved REMPI-ZEKE spectra of para- and ortho- NH_3 (Habenicht *et al.* 1991).

3.4. Ab initio *approaches to rotational line intensities in photoelectron spectroscopy*

Rotational line intensities are calculated *ab initio* within the static-exchange frozen-core approximation which is a single configurational approximation and therefore does not consider electronic or spin–orbit autoionization effects. In addition, the method does not treat interactions between bound states and the ionization continua. A detailed description of the method is not intended here and the reader is referred to the original literature (for instance to the work done by Itikawa (1978a, b), McKoy and coworkers (Lucchese *et al.* 1982, Dixit and McKoy 1985, Dixit *et al.* 1985, Wang and McKoy 1991b) and Raseev, Lefebvre-Brion and coworkers (Raseev *et al.* 1978, Lefebvre-Brion 1990a, Mank *et al.* 1991)). We restrict ourselves here to a simplified discussion of the various steps involved in these *ab initio* calculations, pointing out the connection with the model of Buckingham *et al.* (1970) as well as the successes and limitations of this approach.

The photoionization cross-section is first separated into an angular part and a vibronic part. The evaluation of the angular part consists of the calculation of the $Q(j)$ factors by table 3.1 and in the application of the relevant parity selection rule (Dixit and McKoy 1986, Lefebvre-Brion 1990a). The vibronic transition moment is then calculated by separating the vibronic transition moment into a Franck–Condon factor and an electronic transition moment (Note however that this separation is not a necessary step in the procedure (Dixit *et al.* 1984)). A self consistent field (SCF) wavefunction is constructed for the molecular bound state by employing Gaussian or Slater basis orbitals. The ionization is then assumed to be vertical (frozen-core). This assists in the determination of the electrostatic potential exerted by the ionic core on the photoelectron and reduces the problem to the calculation of one-electron integrals between bound and continuum orbitals. The main difficulty resides in the correct evaluation of the exchange potential V_{ex}: indeed, its value depends on the continuum orbital itself. The continuum wavefunction has therefore to be calculated by solving the Schrödinger equation iteratively (Lucchese *et al.* 1982) or by solving a set of additional integro-differential equations simultaneously to the Schrödinger equation (Raseev *et al.* 1980).

These *ab initio* approaches, which include l mixing of the molecular orbital from which the electron is ejected as well as that of the continuum molecular orbital have proved very useful, in the past 15 years, for the characterization of shape-resonances and have correctly accounted for a variety of complex features observed in the photoionization spectra of molecules. Recent applications of these methods to rotationally resolved conventional PE-spectra have led to a satisfactory agreement with experimental results for the few cases in which rotational resolution could be achieved, i.e. in the REMPI-PES spectra of NO (Viswanathan *et al.* 1986, Leahy *et al.* 1991, Wang *et al.* 1991), OH (de Beer *et al.* 1991), HBr (Xie and Zare 1989, Lefebvre-Brion 1990a, Wang and McKoy 1991a). A reasonable agreement with rotational line intensities measured in ZEKE PE spectra has also been obtained in some cases including OH and OD (Wiedmann *et al.* 1992), H_2O (Lee *et al.* 1992a, b), O_2 (Braunstein *et al.* 1992) and HCl (Wang and McKoy 1991b). In addition *ab initio* methods have highlighted the following two effects which can affect ZEKE-rotational line intensities:

(1) The effect of shape resonances

One of the signatures of shape resonances in the photoionization of diatomics is the dependence of the partial wave characteristics of the photoelectron as the internuclear distance is modified (Lefebvre-Brion 1988). Due to a shape resonance occurring near the lowest ionization threshold of O_2 (Braunstein *et al.* (1992) and references therein), the $l=1$ partial wave increases in importance relative to the $l=3$ partial wave with increasing vibrational excitation of the ion, thus favouring ZEKE transitions involving small changes in core rotation ($N^+ - N''$). The *ab initio* calculation of Braunstein *et al.* (1992) confirms this trend and gives a satisfactory explanation of the experimental spectrum (Braunstein *et al.* 1990).

(2) The effect of Cooper minima

The rotationally resolved REMPI-PE spectrum of OH via the D $^2\Sigma^+$ state ($(3p\sigma)^{-1}$ ionization) measured by de Beer *et al.* (1991) is dominated by $N^+ - N'' = 0, \pm 2$ transitions while the simple argument presented in section 3.2. suggests that the spectrum should be dominated by $N^+ - N'' = \pm 1$ transitions for ionization out of this predominantly ($l=1$) Rydberg orbital. The *ab initio* calculation of Stephens and McKoy (1990) shows that the $3p\sigma \rightarrow k\pi (l=2)$ ionization channel which would lead to $N^+ - N'' = \pm 1$ transitions, is suppressed in the energy range investigated due to the formation of a Cooper minimum in the partial ionization cross-section. Cooper minima have not been observed in ZEKE spectroscopy yet, but could in principle affect ZEKE rotational line intensities in a variety of molecular systems.

A serious limitation of these *ab initio* approaches is that they do not account for autoionization effects in photoionization, a consequence of the single-configurational approximation made in the evaluation of the bound–free transition moment, and of the fact that interactions between bound states and the ionization continua are not considered. The difficulties are illustrated in figure 3.1 by the ZEKE rotational line intensities of the simplest molecular system, H_2 (Merkt and Softley 1992a). Although an *ab initio* calculation of transition moments in the threshold region has not yet been performed, the higher energy calculations of Itikawa (1978b) should be applicable to the region probed by the ZEKE experiment, assuming no Cooper minima or shape resonance. A comparison of the ZEKE spectrum of

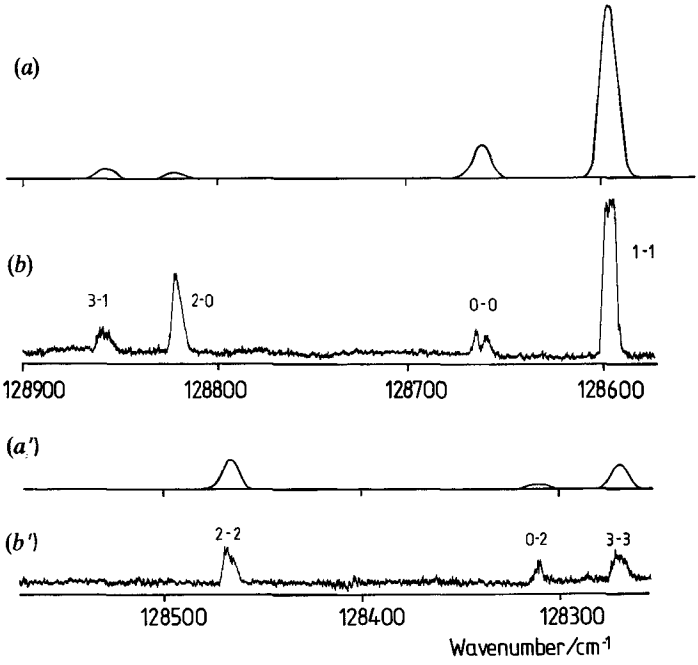

Figure 3.1. (*a*) Predicted ZEKE photoelectron spectrum of the $X\,^2\Sigma_g^+$ ($v^+=2$)←$X\,^1\Sigma_g^+(v=0)$ band of H_2, based on theoretical predictions of rotational linestrengths by Itikawa (1978b), weighted by population factors (298 K) and convoluted with the experimental linewidth. (*b*) Experimental ZEKE photoelectron spectrum of the same band, recorded with $E_1 = 0{\cdot}5\ \mathrm{V\,cm^{-1}}$ and $E_2 = 8\ \mathrm{V\,cm^{-1}}$. The lines are labelled (N^+–J'') where N^+ and J″ refer to the rotational quantum numbers of the ion and neutral respectively. With permission from the American Institute of Physics.

the $X\,^2\Sigma_g^+(v^+=2)$–$X\,^1\Sigma_g^+(v=0)$ ionizing transition of H_2 (figure 3.1 (*b*)) with predictions based on the *ab initio* calculations of Itikawa (1978b) reveals that, while the intensities of the (1–1), (2–2), (3–3) and (3–1) transitions (the notation corresponds to (N^+–J'')) are in good agreement with the theoretical predictions, some clear differences exist between theory and experiment for the (2–0), (0–0) and (0–2) transitions. This disaccord is further illustrated in table 3.2 which shows a comparison between the ZEKE-intensities (column 2), intensities derived from the conventional photoelectron spectra of Åsbrink (1970) (column 3) and Morioka *et al.* (1980) (column 4) intensities calculated *ab initio* by Itikawa (1978b) (column 5) and values calculated from the unperturbed ZEKE-PES transitions by the fitting procedure of Xie and Zare (1992) (column 6). The origin of the perturbed ZEKE transitions can be unambiguously attributed to autoionization by comparing the ZEKE spectrum with high resolution absorption spectrum reported by Herzberg and Jungen (1972): the dip occurring in the middle of the (0–0) transition is a manifestation of a window resonance (see section 4); the enhanced intensity and the narrowness of the (0–2) transition can be attributed to rotational autoionization, while the large intensity of the (2–0) transition is due to complex resonance (see section 4). Autoionization is a general phenomenon affecting most molecular systems, and its marked effect on the ZEKE spectrum of H_2 suggests that it should also be observable in other systems. It will be shown in the following section that autoionization is indeed of fundamental importance in ZEKE-photoelectron spectroscopy.

Table 3.2. Rotational line intensities from the one-photon ionization of H_2 at room temperature.

Transition	Merkt and Softley (1992a) ZEKE-PES	Åsbrink (1970) Ne I-PES	Morioka *et al.* (1980) He I-PES	Itikawa (1978b) *ab initio*	Xie and Zare (1992) Fit.
0–0	15	42	27	18·5	18
2–0	51	6·2	10·5	2·81	3·2
1–1	100	100	100	100	100
3–1	9·5	4·5	—	8·59	9·7
0–2	8·3	2·2	—	0·51	0·6
2–2	20	31	21	17·5	18
1–3	—	—	—	0·5	0·6
3–3	16	15	14	13·3	14
5–3	1·1	—	—	0·93	1·1

4. Autoionization in ZEKE-photoelectron spectroscopy

4.1. *General considerations*

As pointed out in section 3.1., the evaluation of ZEKE line intensities is in essence a multichannel problem. The channel interactions which give rise to intensity distortion in ZEKE-PES are not strictly speaking autoionization processes as they take place between two bound channels rather than between a bound state and a continuum. Nevertheless there is a strong analogy with autoionization, as the Rydberg states detected in a PFI-ZEKE experiment form a pseudo-continuum of states. This pseudo-continuum is turned into a real continuum when the pulsed electric field is applied. The process by which an electron is released as a result of a channel interaction between a discrete Rydberg state and a pseudo-continuum of high Rydberg states and the subsequent field ionization of these high Rydberg states is well known in atomic physics (Garton *et al.* 1962) and has been termed 'forced autoionization' (autoionization cannot occur as long as the ionization threshold is not lowered by the electric field and is therefore 'forced' by the electric field). When the term autoionization is used in this section, it will be meant in a broad sense which includes forced autoionization.

The interactions which can take place between bound and open channels near a specific ionization threshold are shown in figure 4.1 in which the A_i represent discrete Rydberg states of moderate to low principal quantum number n, B stands for the pseudo-continuum of high Rydberg states which are detected in a ZEKE-PFI experiment and the A_μ for the open channels, which can be dissociation or ionization continua. The interactions between the different channels are indicated by arrows and the label I_i, I_μ or $I_{i\mu}$ for interactions A_i–B, B–A_μ and A_i–A_μ respectively. Interactions of the type A_i–A_j are not considered explicitly in figure 4.1. This does not lead to a loss of generality of the picture as the bound states A_i can be considered as prediagonalized. Interactions between the open channels A_μ caused by the anistropy of the molecular core potential (these interactions lead to l mixing of the free electron wavefunction (Rudolph *et al.* (1988a, b), see also section 3.3. and 3.4. above) are not considered either. Instead, each A_μ channel is considered as a mixture of different l components. In general, the prediction of ZEKE line intensities requires the knowledge of the

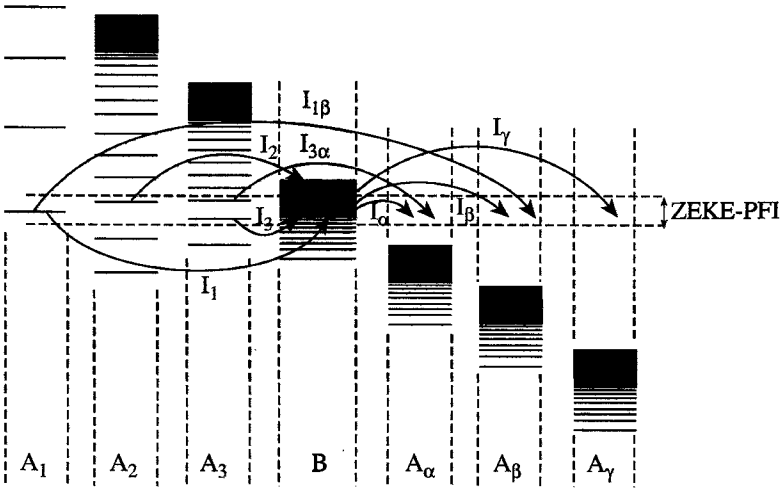

Figure 4.1. Illustration of the channel interactions which take place in the vicinity of an ionization threshold and which are important in ZEKE-PES. Details are given in the text.

magnitude of all the interactions represented in figure 4.1 and of all the transition moments from the neutral ground state to the final states A_i, A_μ and B, as well as the evaluation of the evolution of the system from the time of excitation until the application of the field-ionizing electric field, a potentially formidable task. Fortunately, an important approximation can often be used to reduce the complexity of the problem. It consists of neglecting all interactions I_μ between the high Rydberg states B and the open channels A_μ. Were these interactions significant, ionization would occur on a relatively short timescale compared to the typical delay time of 1 μs (or longer) between excitation and field-ionization in ZEKE spectroscopy. As a result, no ZEKE signal would be observed, in evident contrast to the large bulk of ZEKE data obtained to date by delayed pulsed field ionization (PFI). The very fact that any ZEKE signal can be detected at all by PFI 1 μs after ionization *implies* the weakness of the I_μ interactions in figure 4.1.

As demonstrated with much insight by Chupka (1992), lifetimes of 1 μs for the high n Rydberg states detected in ZEKE experiments cannot be rationalized in terms only of the long orbiting period of the Rydberg electrons. It is well-known that even a small stray electric field (<100 mV/cm), as is always present in ZEKE experiments, can induce complete Stark mixing of high Rydberg states lying a few cm^{-1} below an ionization threshold. In the presence of a stray electric field, or of a weak applied d.c. field, these high Rydberg states contain a significant high-l (i.e. non-penetrating) character. As a result they interact less with the ionic core and are more resistant to autoionization. l mixing by a weak electric field (note the difference with the l-mixing caused by the anisotropy of the molecular core potential) therefore weakens the I_μ interactions and increases the lifetime of high Rydberg states. Chupka (1992) also points out that collisional processes could contribute to l mixing and to the randomization of m_l. The latter effect gives an addtional weight of $(2l+1)$ to non-penetrating high-l components and therefore significantly prolongs the lifetime of the high-n Rydberg states detected in PFI-ZEKE experiments.

It should be pointed out here that the assumption of long lifetimes (which is equivalent to neglecting I_μ) is only valid for the highest Rydberg states ($n>100$) and does not apply to lower Rydberg states which are far less sensitive to external electric fields and collisional processes. In fact, it turns out, in the cases of Ar, N_2 and H_2, that when the ZEKE detection band, defined by the magnitudes of E_1 and E_2 according to equation (2), is tuned below 25 cm^{-1} underneath a threshold no ZEKE signal can be detected by delayed (1 μs) PFI (Merkt and Softley 1992c).

Considering the remaining interactions I_i and $I_{i\mu}$ in figure 4.1 and the transition matrix elements μ_{iX} and μ_{BX} from the ground state X to the A_i and B channels leads to a series of limiting cases which are important for ZEKE spectroscopy and which are discussed here in turn:

(1) $I_i=0$.

The ZEKE rotational line intensities are governed by direction ionization (see section 3).

(2) $I_i\neq 0$, $\quad \mu_{iX} \gg \mu_{BX}$.

The ZEKE rotational line is affected by an autoionization resonance and borrows intensity from the strong A_i–X transition: it appears more intense than predicted by considering direct ionization only. These autoionization resonances can appear anywhere within the ZEKE bandwidth and can cause the ZEKE-line to be sharper than predicted by equation (2). The shape of these

autoionization resonances correspond to a Fano profile (Fano 1961, 1970) with a large q factor. This situation has already been encountered in the ZEKE spectra of a wide range of molecules and will be discussed in detail in subsections 4.2. to 4.5.

(3) $I_i \neq 0, \quad \mu_{iX} \ll \mu_{BX}$.

The interaction between the A_i and B channels leads to a reduction of the ZEKE line intensity. A so called window resonance is observed, that is to say an autoionization dip corresponding to a Fano profile with a small q factor. Such a situation has so far only been unambiguously observed in the ZEKE spectrum of H_2 (Merkt and Softley 1992a) but should be observable in other ZEKE-spectra. Window resonances are a common phenomenon in photoionization.

(4) $I_{i\mu} \gg I_i$.

The discrete states belonging to the A_i channels are coupled very strongly to the open channels A_μ (for instance to the dissociation continua) but only weakly to the B channel. They are short-lived and considerably broadened and therefore hardly affect the ZEKE line intensities (Chupka 1992). Here again, the ZEKE intensities are governed by direct ionization.

(5) No discrete state lies in the ZEKE detection bandwidth.

This situation becomes more and more probable as the PFI–ZEKE detection bandwidth is minimized. It is also more likely to be encountered in molecular systems with large spacings between adjacent ionic rotational and vibrational levels, as the density of discrete autoionizing Rydberg states converging to higher rovibrational levels of the ion will be small in the vicinity of a given ionization threshold. However, even the ZEKE spectrum of H_2 (H_2^+ has only one mode of vibration with a large vibrational constant ($\omega_e \cong 2320\,\mathrm{cm}^{-1}$) and the largest rotational constant of all molecular ions ($B_e \cong 30\,\mathrm{cm}^{-1}$)) is significantly perturbed by autoionization (see figure 3.1 and sections 4.2. and 4.4. below). Other systems with large rotational spacings, like HCl (Haber *et al.* 1991, Tonkyn *et al.* 1992) and OH (Wiedmann *et al.* 1992), are also influenced by autoionization.

Intermediate cases are likely to be encountered in many systems. In the ZEKE spectra of the X ($v^+ = 1$ and 2) states of N_2^+, for instance (Merkt and Softley 1992b, Wilson *et al.* 1992), the ZEKE line intensities appear to be strongly affected by one or more autoionizing Rydberg states converging to the A state of N_2^+. These states are not only strongly coupled to the ZEKE pseudo continua of high Rydberg states, but also to a large series of open continua and the situation is intermediate between limiting cases (3) and (4). The ZEKE intensities can be treated in analogy to case (3) but must be weighted by the factor

$$\frac{I_i}{\sum_\mu I_{i\mu}}.$$

To summarize, the dynamical behaviour of a ZEKE experiment appears to be as follows: population of high-n, low-l Rydberg states occurs either by direct excitation or indirectly through channel interaction. As soon as the molecular system is in such a high-n, low-l Rydberg state, very fast l mixing (and possibly m_l mixing (Chupka 1992)) occurs and the electron is 'trapped' in long-lived, non-penetrating orbitals and has to wait for the field ionizing pulse before it can escape. This behaviour is only expected in the range of high Rydberg states down to approximately $25\,\mathrm{cm}^{-1}$ below each ionization threshold, i.e. in the region when l and m_l mixing is significant.

4.2. *Rotational autoionization*

4.2.1. *Introduction*

Rotational autoionization is by far the most widely encountered autoionization phenomenon in ZEKE-PE spectroscopy. It has so far been observed in the ZEKE spectra of a wide range of diatomic and triatomic molecules including NO (Takahashi *et al.* 1991, Reiser and Müller-Dethlefs 1992), N_2O (Wiedmann *et al.* 1991), NO_2 (Bryant *et al.* 1992), N_2 (Merkt and Softley 1992b), H_2 (Merkt and Softley 1992a), Na_2 (Bühler 1990, Bühler and Gerber 1992), OH (Wiedmann *et al.* 1992), HCl (Haber *et al.* 1991, Tonkyn *et al.* 1992, Zhu *et al.* 1992), and possibly in other systems like H_2O (Gilbert and Child 1991, Tonkyn *et al.* 1991, Lee *et al.* 1992a) and H_2S (Wiedmann and White 1992). It has not yet been conclusively observed in systems with more than three atoms. Several reasons can be invoked for this: first, rotational resolution is difficult to achieve in large systems which generally have small rotational constants; it has so far not been obtained for any system larger than benzene (Chewter *et al.* 1987). Secondly, the large number of vibrational modes some of which have low frequencies, leads to a significantly higher density of discrete Rydberg states in the vicinity of the ionization thresholds and rotational autoionization could be easily overshadowed by other processes. Finally, predissociation probably plays a more important role in large systems.

The reason for the frequent occurrence of rotational autoionization in ZEKE spectroscopy compared with other types of autoionization can be linked directly to the fact that the spacing between adjacent ionic rotational levels is generally much smaller than that separating vibrational and electronic states. Consequently, the density of Rydberg states which can rotationally autoionize in the vicinity of a given threshold is much higher than the density of vibrationally or electronically autoionizing states. For the same reason, rotational autoionization is more likely to occur in systems with small rotational constants. One should also note that jet-cooled samples, in which only a restricted number of rotational levels are populated in the ground state, are less likely to be subject to rotational autoionization than warm samples because the lowest ionic rotational levels have few or no degenerate continua of lower core rotational quantum numbers. The observation of rotational autoionization is also less probable when ionization is achieved by REMPI, because the selection of a specific intermediate rovibronic state in the REMPI process restricts the excitation to a limited number of channels and the ZEKE spectrum to a short series of lines; in contrast, long rotational progressions can be observed by one-photon ionization.

Gilbert and Child (1991) were the first to investigate theoretically the effects of rotational autoionization on ZEKE line intensities. Further theoretical work is currently in progress in other groups; particularly promising seems to be a combination of *ab initio* and MQDT calculations (Lefebvre-Brion 1992).

The conditions for rotational autoionization have been outlined in section 4.1. (cases 2 and 3) and the process can lead to either a window resonance or an autoionization peak. The mechanism of rotational autoionization is illustrated in figure 4.2 for the particular case of the N_2 molecule (Merkt and Softley 1992b). Excitation from a given rotational level (here $J'' = 12$) of the ground vibronic state of N_2 takes place predominantly to the Rydberg series converging to the ($N^+ = J''$) level of the ion, while transitions to Rydberg states converging on ($N^+ \neq J''$) limits are weak (Johns 1974). In addition, transitions for which the difference ($N^+ - J''$) is odd are forbidden by the parity selection rule. These Rydberg states converging to the ($N^+ = J''$) limits are coupled to the pseudo-continuum of high Rydberg states

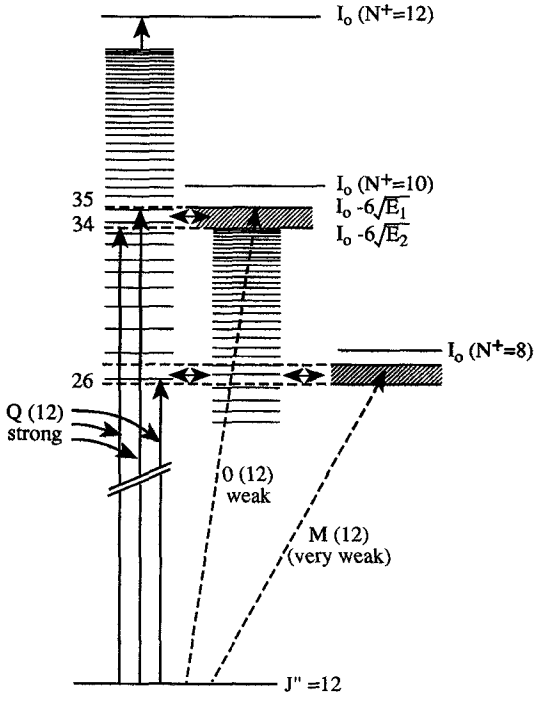

Figure 4.2. Rotational autoionization mechanism explaining how weak O- and M-ZEKE transitions can borrow intensity from strong Q transitions to Rydberg states converging on other limits. The mechanism involves a coupling between low (n=20–60) Rydberg states converging to the ($N^+ = J''$) rotational levels of the ion and high Rydberg states ($n > 100$) converging to ($N^+ = J'' - 2$) rotational levels of the ion, where j is a positive integer. With permission from the American Institute of Physics.

converging on lower N_f^+ limits (here $N_f^+ = 10, 8, \ldots$) and the situation corresponds to case 2 of section 4.1. In the case of a $\Delta N^+ = -2$ interaction, $N_f^+ = 10$, and rotational autoionization leads to an enhancement of the ZEKE transitions with $N^+ J'' - 2$, also referred to as O-branch lines. In the case of a $\Delta N^+ = -4$ interaction, $N_f^+ = 8$, and rotational autoionization leads to an enhancement of the ZEKE transitions with $N^+ = J'' - 4$, or M-branch lines.

The usual signature of rotational autoionization in ZEKE spectra is a difference in the intensity of rotational branches corresponding to a negative change in core rotation compared to branches corresponding to a positive change in core rotation of the same magnitude. Such an asymmetry has been noticed in N_2O (Wiedmann *et al.* 1991, Bryant *et al.* 1992), HCl (Tonkyn *et al.* 1992), NO (Takahashi *et al.* 1991, Reiser and Müller-Dethlefs 1992), OH (Wiedmann *et al.* 1992) and N_2 (Merkt and Softley 1992b). The reason for this asymmetry can be immediately seen from figure 4.2: while O- and M-branch intensities can be enhanced, as discussed above, the intensity of S branches (with $N^+ = J'' + 2$) or U branches (with $N^+ = J'' + 4$) cannot, as the high Rydberg states just below the $N^+ = 14$ and $N^+ = 16$ states are degenerate with the *continuum* above the $N^+ = 12$ threshold.

In some favourable cases, single autoionizing Rydberg states can be resolved in ZEKE spectra as is the case in the ZEKE spectra of H_2 (Merkt and Softley 1992a), N_2 (Merkt and Softley 1992b), Na_2 (Bühler and Gerber 1992), HCl (Haber *et al.* 1991) and

NO_2 (Bryant *et al.* 1992). These cases are of particular importance as they provide considerable details on the process of rotational autoionization, in particular propensity rules for rotational autoionization. For simplicity we concentrate here on the series H_2, N_2 and Na_2 for which symmetry constrains the changes of N^+ to be even numbered.

4.2.2. *Rotational autoionization in the ZEKE spectrum of H_2*

As mentioned at the end of section 3, two rotational lines of the ZEKE spectrum of the X $^2\Sigma_g^+(v^+=2)$–X $^1\Sigma_g^+(v=0)$ ionizing transition of H_2 are perturbed by rotational autoionization. These lines are labelled (0–0) and (0–2) in figure 3.1 and table 3.2 according to the notation (N^+–J''). The (0–0) transition is an example of a window resonance (case 3 in section 4.1.). The position of the dip in the profile of this line (figure 3.1) is independent of the magnitude of the electric fields E_1 and E_2 (see equation (2)) used in the ZEKE experiment as can be seen in figure 4.3, and is in complete accord with the results of Herzberg and Jungen (1972) and Dehmer and Chupka (1976) who observed this window resonance in the absorption and photoionization spectrum respectively. Figure 4.3 is also an illustration of the flexibility and the power of the ZEKE method for the study regions of controlled energy and width in the vicinity of ionization thresholds.

The mechanism leading to the narrow width and enhanced intensity of the (0–2) transition comes from the same channel interaction as in the case of the (0–0) transition, but the situation corresponds now to case 2 of section 4.1. Both mechanisms are illustrated in figure 4.4 and the reader is referred to the original literature (Herzberg and Jungen 1972, Merkt and Softley 1992a) for additional details. The selection rule for rotational autoionization in H_2 is $\Delta N^+ = -2$ (Herzberg and Jungen 1972, Dehmer and Chupka 1976, Xu *et al.* 1988, Merkt and Softley 1992a).

4.2.3. *Rotational autoionization in the ZEKE spectrum of N_2*

The ZEKE-PE spectrum of the X $^2\Sigma_g^+(v^+=0)$–X $^1\Sigma_g^+(v=0)$ transition of N_2 is represented in figure 4.5. The intensity of the O and M branches ($N^+ - J'' = -2$ and -4 respectively) is much larger than that of the S and U branches (N^+–$J'' = 2$ and 4) and is indicative of rotational autoionization (figure 4.2). The irregularities in the intensities within the O and M branches of this spectrum are another signature of rotational autoionization. The situation in N_2 is more complex than in H_2 due to the smaller value of the molecular rotational constant ($2\,cm^{-1}$ compared with $60\,cm^{-1}$) and ionic rotational constants ($2\,cm^{-1}$ compared with $30\,cm^{-1}$). First, more rotational levels are populated in the ground state at room temperature and, secondly, the small separation between adjacent ionic rotational levels leads to a much higher density of autoionizing Rydberg states. Measurement of the ZEKE spectrum at different extraction voltages, following the same method as that used in figure 4.3, however, leads to the complete resolution and the assignment of a large number of rotationally autoionizing Rydberg states (Merkt and Softley 1992b).

Figure 4.6 illustrates the considerable information which can be gained from such experiments: the experimental ZEKE spectrum measured with an extraction field of $6\,V\,(cm)^{-1}$ applied 500 ns after excitation is represented below a simple simulation of the spectrum (the reader is referred to (Merkt and Softley 1992b) for more details). The rotationally autoionizing Rydberg states are labelled N^+/n, and an additional branch label (O, M and K) indicates that the autoionization process corresponds to ΔN^+ changes of -2, -4 and -6 respectively. The propensity rules for rotational

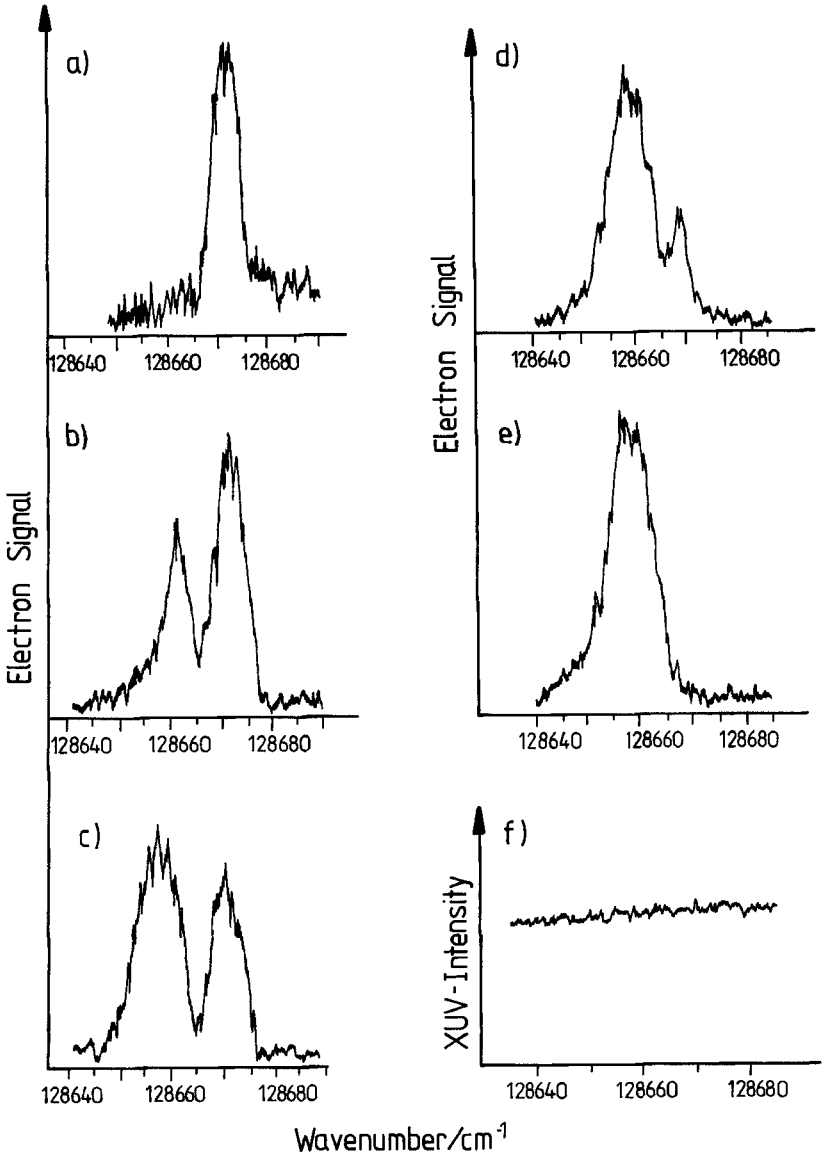

Figure 4.3. Effect of different combinations of discrimination (E_1) and extraction (E_2) fields on the profile of the (0–0) transition in the ZEKE spectrum of H_2. (E_1/E_2 in V (cm)$^{-1}$). (*a*) 0/4 (*b*) 0/8 (*c*) 0/12 (*d*) 1/12 (*e*) 1·5/12. The position of the dip in (*b*), (*c*), and (*d*) does not change with E_1 and E_2. The XUV generation profile shown in (*f*) has no corresponding dip. With permission from the American Institute of Physics.

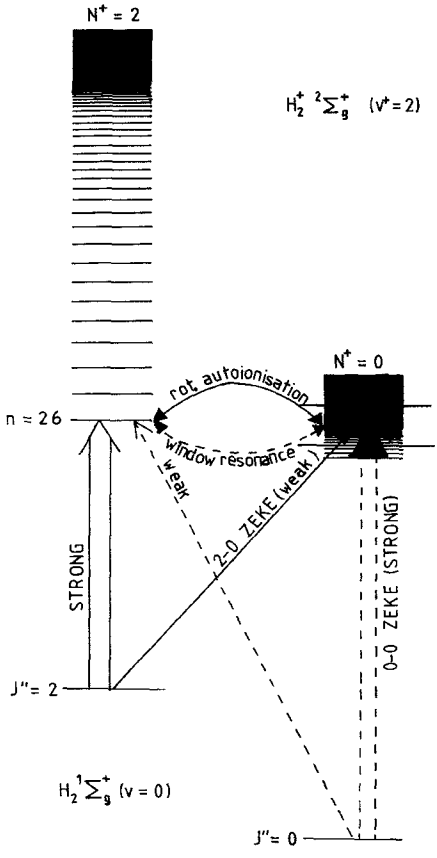

Figure 4.4. Rotational autoionization in H_2. The diagram shows how the interaction between the $n=26$ Rydberg state belonging to the series converging to the $v^+=2$, $N^+=2$ state of the H_2^+ and the pseudo-continuum of high Rydberg states just below the $N^+=0$ state leads to a window resonance in the (0–0) ZEKE line (dotted lines) and to an autoionization peak in the (0–2) ZEKE line (full lines).

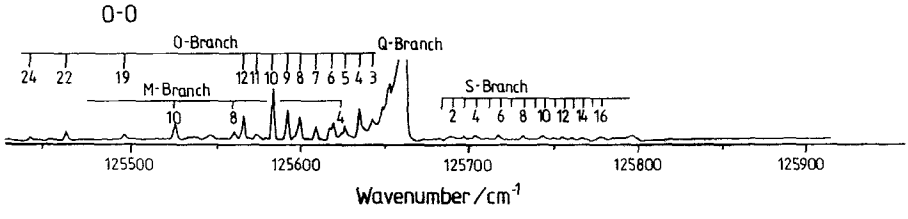

Figure 4.5. ZEKE-photoelectron spectrum of the $X\,^2\Sigma_g^+$ $(v^+=0)\leftarrow X\,^1\Sigma_g^+(v^+=0)$ band of N_2, recorded with an extraction field of 1 V $(cm)^{-1}$ applied 500 ns after excitation. The branch labels M, O, Q and S refer to the difference (N^+-J'') between ionic and neutral rotational quantum numbers.

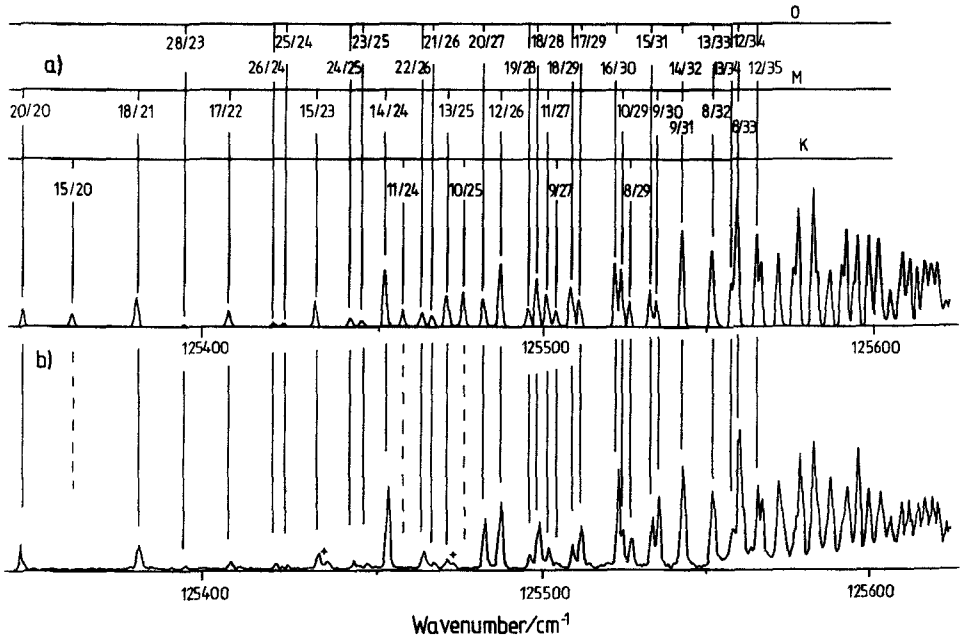

Figure 4.6. Simulated (*a*) and experimental (*b*) ZEKE rotational autoionization spectra of N_2 near the $X\,^2\Sigma_g^+$ ($v^+=0$) threshold corresponding to an extraction field of 6 V (cm)$^{-1}$. The lines are labelled with N^+/n where $N^+=J''$ is the rotational angular momentum of ion-core and n in Rydberg principal quantum number. A further label O, M or K indicates that the autoionization process involves changes in the core rotational quantum number N^+ of -2, -4 and -6 respectively. With permission from the American Institute of Physics.

autoionization derived from the spectrum are $\Delta N^+=-2\ -4$, and, to a lesser extent, -6. It is interesting to note that window resonances are not observed in the ZEKE spectrum of N_2. They would be expected to cause dips in the profile of Q-branch transitions (with $N^+=J''$). Unfortunately, Q-branch lines are too closely spaced in the ZEKE spectrum and the superposition of many line hampers the resolution of window resonances. These would probably be observable in a $(1+1')$ or $(2+1')$ REMPI experiment.

4.2.4. *Rotational autoionization in the ZEKE spectrum of Na_2*

The Na_2 molecule provides a further example in the series of homonuclear diatomic molecules of decreasing rotational constants. The rotational constant of Na_2^+ (0·113 cm^{-1} (Martin *et al.* 1982)) is approximately 20 times smaller than that of N_2^+ and 260 times smaller than that of H_2^+. Resolving the rotational structure in the ZEKE spectrum of Na_2 requires the use of REMPI excitation methods. Figure 4.7 represents the ZEKE spectrum measured by Bühler (Bühler 1990, Bühler and Gerber 1992). These authors use a $(1+1')$ REMPI excitation scheme in which the pump laser excites to the $v'=0$, $J'=11$ level of the A state of Na_2, and the probe laser induces the sequential excitation from this selected intermediate state to various rotational levels of the ground vibronic state of ion. The spectrum shows the expected asymmetry in intensity between $(N^+-J'<0)$ and $(N^+-J'>0)$ lines. In addition, a clear series of partially

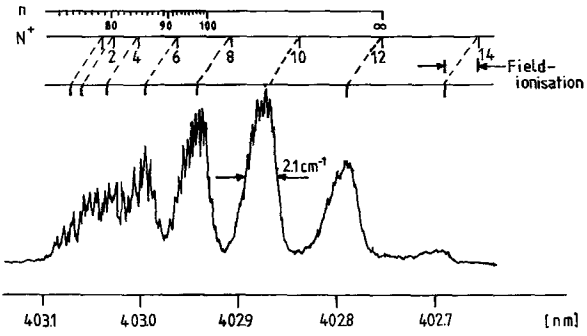

Figure 4.7. REMPI-ZEKE photoelectron spectrum of the X ($v^+ = 0$) state of Na_2^+. Ionization occurs from the selected A ($v' = 0, J' = 11$) intermediate level. Adapted from Bühler (1990).

resolved Rydberg states converging to the $N^+ = 12$ level of the ion confirms that the enhanced intensity of the ($N^+ - J' < 0$) transitions originates from rotational autoionization. The propensity rules for rotational autoionization in Na_2, $\Delta N^+ = -2$, $-4, \ldots, -12$ (and possibly larger), can be immediately derived from the spectrum.

4.2.5. *The importance of electric fields*

The large ΔN^+ changes observed in the rotational autoionization/ZEKE spectrum of Na_2 compared to those observed in H_2 and N_2 is surprising at first sight, but compatible with the findings of Bordas *et al.* (1987) and Mahon *et al.* (1990) who measured ΔN^+ changes of up to -20 and -10 in Na_2 and Li_2 respectively, by observing the lowering of the ionization thresholds caused by field-induced rotational autoionization. In both cases, it is demonstrated that electric fields induce the large ΔN^+ changes observed experimentally. Bordas *et al.* (1987) invoke J mixing caused by the electric field, whereas Mahon *et al.* (1990) propose a multistep autoionization mechanism based on l mixing.

The differences in behaviour between Na_2 and Li_2 on the one hand, and N_2 and H_2 on the other, can also be explained qualitatively by the effects of electric fields, as such effects are expected to be particularly important for ions with small rotational constants (like Na_2^+ and Li_2^+): indeed, in such systems, the Rydberg states which autoionize rotationally have much higher principal quantum numbers n and are therefore more sensitive to weak external electric fields. These trends are confirmed by a recent calculation which also demonstrates the differences between J and l mixing (Merkt *et al.* 1992a).

4.3. *Spin–orbit autoionization*

Long-lived ($\tau > 5\,\mu s$) Rydberg states belonging to series converging to both spin–orbit components of the X $^2\Pi$ ground state of HCl^+ have been studied experimentally by Haber *et al.* (1991) by pulsed field ionization some $5\,\mu s$ after excitation. Excitation to the Rydberg states detected in the experiment was achieved in a two colour experiment, via the $J' = 2$ level of the 4pπ F $^1\Delta$ Rydberg state. The PFI spectrum reveals extensive progressions of autoionizing Rydberg states, starting with relatively low n values, which converge to the various accessible rotational levels of both spin–orbit components of the ion, revealing the importance of both rotational and spin–orbit autoionization on the spectrum. Most of the autoionization structure

disappears from the PFI-ZEKE spectrum when a discrimination field of 500 mV $(cm)^{-1}$ is applied prior to the extraction (extraction field 2 V $(cm)^{-1}$), which suggests that the coupling between the different channels that leads to autoionization is induced by the presence of an electric field (Haber *et al.* 1991).

More recent experimental and theoretical investigations of the same system (Zhu *et al.* 1992) show the importance of spin–orbit autoionization on ZEKE line intensities more quantitively: the intensity ratio $I(^2\Pi_{1/2})/I(^2\Pi_{3/2})$ is 0·56, i.e. approximately half that one would expect from the equal degeneracy of the two spin–orbit components. This indicates that the $^2\Pi_{3/2}$ component gains intensity from spin–orbit autoionization of Rydberg states converging to the upper $^2\Pi_{1/2}$ component.

The importance of spin–orbit and rotational autoionization in the threshold photoelectron spectrum of the same states has also been demonstrated by Frohlich *et al* (1991).

4.4. *Vibrational autoionization*

Vibrational autoionization in ZEKE-PES has so far only been conclusively observed in the ZEKE spectrum of H_2 (Merkt and Softley 1992a). The unexpectedly large intensity of the rotational (2–0) line of the X–X ionizing transition was noted at the end of section 3 (figure 3.1, table 3.2) and can be attributed to a coupling between the $n=8, l=1$ Rydberg state, belonging to the series converging to the $v^+=3, N^+=0$ state of the ion and the pseudo-continuum of high Rydberg states converging to the $v^+=2$, $N^+=2$ limit. A comparison between the prompt autoionization spectrum, recorded by measuring the electrons sent to the detector by the discrimination electric field, and the ZEKE-spectrum is shown in figure 4.8. The complicated structure seen at the right of figure 4.8 (*b*) at 128 790 cm^{-1} is an example of a complex resonance (Jungen and Raoult 1981): the $v^+=3$, $R(1)$ 8p1 resonance interacts with the transitions to high Rydberg states converging to the $v^+=2, N^+=3$ limit. This limit corresponds to the (3–1) ZEKE peak in figure 4.8 (*a*). The mechanism for the enhancement of the (2–0) ZEKE transition described above is therefore similar to that leading to a complex resonance.

4.5. *Electronic autoionization*

Electronic autoionization effects on ZEKE line intensities are only expected for ions having low-lying electronic states and should therefore not play a significant role

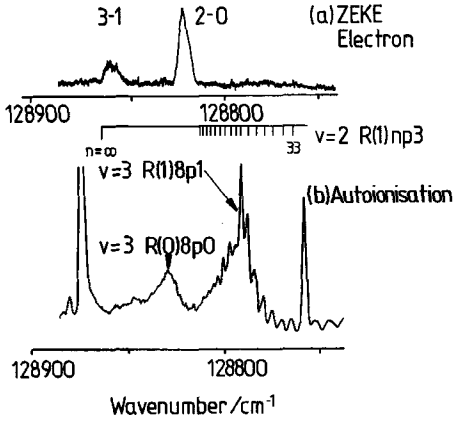

Figure 4.8. (*a*) ZEKE photoelectron spectrum of H_2 reproduced from figure 3.1. (*b*) 'Autoionization spectrum' of H_2, recorded by collecting the electrons sent to the detector by the discrimination field E_1. With permission from the American Institute of Physics.

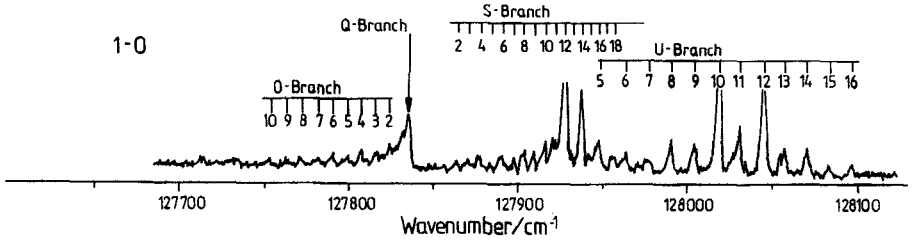

Figure 4.9. ZEKE-photoelectron spectrum of the $X\,^2\Sigma_g^+(v^+=1) \leftarrow X\,^1\Sigma_g^+(v=0)$ band of N_2, recorded with an extraction field of 1 V (cm)$^{-1}$ applied 500 ns after excitation. The branch labels O, Q, S and U refer to the difference ($N^+ - J''$) between ionic and neutral rotational quantum numbers.

in the ZEKE spectra of most simple molecules like for instance O_2, NO, H_2, CO, HF, HCl, OH. N_2 represents an important exception as the A state of N_2^+ lies only $\approx 9000\,cm^{-1}$ above the ground electronic state and the density of Rydberg states converging to the various vibrational levels of the A state is significant in the region of the X state of N_2^+. Electronic autoionization is expected to have an influence on ZEKE rotational line intensities of the X–X transition, and particularly so in a room temperature spectrum. (The ZEKE-PE spectrum of P_2 should be even more subject to the effects of electronic autoionization, as the $A\,^2\Sigma_g^+$-state of P_2^+ lies only $\approx 2000\,cm^{-1}$ above the ground electronic state ($X\,^2\Pi_u$.) The ZEKE spectrum of the $X\,^2\Sigma_g^+(v^+=1) - X\,^1\Sigma_g^+(v=0)$ band of N_2 is displayed in figure 4.9. The large intensities of the S and U branches and the fact that the two pairs of lines (S(12), U(10)) and (S(14), U(12)) are particularly strong betrays a channel interaction. The spectrum can be qualitatively accounted for by a model based on an interaction between the high Rydberg states converging to the rotational levels of the $v^+=1$ level of the X state and an as yet unassigned Rydberg state belonging to a series converging to the A state (Merkt and Softley 1992 *b*). A more quantitative interpretation of this spectrum and of that of the $v^+=2$ state, which contains similar effects, is in progress (Wilson *et al.* 1992).

5. Conclusions

This article has reviewed recent advances in the understanding of ZEKE rotational line intensities. Several aspects remain unclear and require further experimental and theoretical work.

Ab initio calculations of ZEKE-rotational line intensities which do not take autoionization into account appear to successfully reproduce experimental results in a number of systems (table 5.1). In these systems direct ionization is dominant. At the same time, abnormal intensity patterns which can be unambiguously attributed to autoionization have been identified in the ZEKE spectra of a wide range of molecules (table 5.2). It is not absolutely clear why autoionization plays a role in some systems only. Several factors, already mentioned in section 4, can be suggested by comparing tables 5.1 and 5.2: autoionization seems to be more readily observed in ZEKE spectra of warm gas samples than in jet cooled ones, a consequence of the wider range of states sampled. For the same reason, one would expect REMPI-ZEKE spectra to be less marked by autoionization effects than one-photon ZEKE spectra. The width of the ZEKE detection band (equations (1) and (2)) is also expected to be of crucial importance: the wider it is, the more probable it is that an autoionizing Rydberg state will perturb the intensity of a given ZEKE-line. This is illustrated in figure 4.3, where

the effect of the window resonance on the (0–0) transition of the ZEKE spectrum of H_2 can be avoided by an appropriate choice of extraction fields as in figure 4.3 (*a*). Similarly, the interaction width should play an important role: for instance, the *R*(0)8p0 transition, which leads to the enhancement of the (2–0) ZEKE transition in H_2 by the complex resonance mechanism discussed in Subsection 4.4, lies several cm^{-1} on blue side of the ZEKE line (figure 4.8) but the overall profile of the complex resonance is wide enough to affect its intensity.

Until very recently, the factors leading to the long lifetimes of the Rydberg states detected in a ZEKE experiment were not well understood. The most satisfactory explanation so far is that of l and m_l mixing induced by electric fields and collisional processes discussed by Chupka (1992). In that context, it will be of particular interest, in future, to determine how far below a given threshold Rydberg states are subject to these effects. This could be done by measuring the lifetime of these Rydberg state as a function of n, for instance by measuring ZEKE spectra at a wide range of delay times, and for a wide range of discrimination and extraction fields (E_1 and E_2 in equation (2)). Also, a variation of the pressure of the molecular sample might reveal the importance of collisional processes, in particular that of m_l mixing.

In cases where the timescale of the interaction which leads to autoionization is of the order of a microsecond, a variation of the delay time between excitation and field ionization might provide some very useful dynamical information.

An important consequence of the dynamical picture of a ZEKE experiment proposed in the last paragraph of Subsection 4.1 is that, once the photoelectron is 'trapped' in long-lived, non-penetrating high-l and high-n Rydberg orbitals, *it will be insensitive to the motion of the ionic core and will act as a spectator to eventual changes of the nuclear configuration.* Recent results obtained on the A–X ionizing transition of CO clearly indicate that the Rydberg states detected by PFI ZEKE-PES survive 1 μs, i.e. longer than the fluorescence lifetime of the ion core (Hepburn 1992). Fluorescence of

Table 5.1. Systems in which ZEKE rotational line intensities are governed by direct ionization

Molecule	Transition	Excitation	Resolution FWHM/cm^{-1}	T/K	Reference
O_2	$X^2\Pi_g \leftarrow X^3\Sigma_g^-$	XUV	2	5–110	Braunstein *et al.* (1992)
H_2O	$X^2B_1 \leftarrow X^1A_1$	XUV	2	15	Lee *et al.* (1992a)
OH[(a)]	$X^3\Sigma^- \leftarrow X^2\Pi$	XUV	3	220 K	Wiedmann *et al.* (1992)
HCl	$X^2\Pi \leftarrow F^1\Delta$	(2+1′) REMPI	5	—	Wang and McKoy (1991b)

(*a*) weak effect of rotational autoionization.

Table 5.2. Systems in which autoionization clearly affects ZEKE line intensities.

Molecule	Transition	Excitation	Resolution FWHM/cm^{-1}	T/K	Reference
H_2	$X^2\Sigma_g^+ \leftarrow X^1\Sigma_g^+$	XUV	1·5–10	RT	Merkt and Softley (1992a)
N_2	$X^2\Sigma_g^+ \leftarrow X^1\Sigma_g^+$	XUV	1·5–10	RT	Merkt and Softley (1992b)
NO_2	$X(100) \leftarrow 3p\sigma\ ^2\Sigma_u^+$	REMPI	5	—	Bryant *et al.* (1992)
N_2O	$X \leftarrow X$	XUV	2	150 K	Wiedmann *et al.* (1991)
HCl	$X^2\Pi_{3/2} \leftarrow X^1\Sigma^+$	XUV	2	300 K	Tonkyn *et al.* (1992)
Na_2	$X \leftarrow A$	REMPI	2	—	Bühler (1990)

the ion core seems therefore to occur without significantly disturbing the Rydberg electron. If this is confirmed, one could further speculate that the ion core might start dissociating without directly influencing the Rydberg electron which could adiabatically follow the ionic fragment. The ZEKE extraction field would then field ionize the fragment rather than the complete molecule. Such an hypothesis could be tested by detecting the field ionized electron in coincidence with the ionic fragment (PFI-ZEKE-PEPICO).

To conclude, it seems fair to say that ZEKE photoelectron spectroscopy does not only provide important data such as ionization potentials and ionic constants, but has also opened completely new perspectives for the spectroscopy and dynamics of high Rydberg states.

Acknowledgments

We are grateful to the SERC and to the Paul Instrument Fund for financial support and to Magdalene College, Cambridge and the Ministère des Affaires Etrangères France, for additional support to one of us (F. M.). We also wish to express our thanks to Professor M. S. Child and Miss H. H. Fielding (Oxford) for discussions and to Professor P. M. Guyon and Professor H. Lefebvre-Brion (Orsay) for useful suggestions and critically reading the manuscript. Finally, we would like to thank Professors W. A. Chupka, E. R. Grant, M. G. White and R. N. Zare for making some of their results available to us before publication.

References

AKULIN, V. M., REISER, G., and SCHLAG, E. W., 1992, *Chem. Phys. Lett.*, **195**, 383.
ALLENDORF, S. W., LEAHY, D. J., JACOBS, D. C., and ZARE, R. N., 1989, *J. chem. Phys.*, **91**, 2216.
ARNOLD, D. W., BRADWORTH, S. E., KISTOPOULOS, T. N., and NEUMARK, D. M., 1991, *J. chem. Phys.*, **95**, 8753.
ÅSBRINK, L., 1970, *Chem. Phys. Lett.*, **7**, 549.
BAER, T., 1986, *Adv. chem. Phys.*, **64**, 111; 1989, *Ann. Rev. phys. Chem.*, **40**, 637.
BAER, T., PEATMAN, W. B., and SCHLAG, E. W., 1969, *Chem. Phys. Lett.*, **4**, 243.
BAER, T., and GUYON, P. M., 1986, *J. chem. Phys.*, **85**, 4765.
BALTZER, P., 1992 (private communication).
BALTZER, P., WANNBERG, B., KARLSSON, L., CARLSSON GÖTHE, M., and LARSSON, M., 1992, *Phys. Rev.* A, **45**, 4374.
BERKOWITZ, J., 1979, *Photoabsorption, Photoionization and Photoelectron Spectroscopy*, (New York: Academic Press).
BORDAS, C., BREVET, P., BROYER, M., CHEVALEYRE, J., and LABASTIE, P., 1987, *Europhys. Lett.*, **3**, 789.
BRAUNSTEIN, M., MCKOY, V., and DIXIT, S. N., 1992, *J. chem. Phys.*, **96**, 5276.
BRAUNSTEIN, M., MCKOY, V., DIXIT, S. N., TONKYN, R. G., and WHITE, M. G., 1991, *J. chem. Phys.*, **93**, 5345.
BRYANT, G. P., JIANG, Y., MARTIN, M., and GRANT, E. R., 1992, *J. phys. Chem.*, **96**, 4827.
BUCKINGHAM, A. D., ORR, B. J., and SICHEL, J. M., 1970, *Phil. Trans. R. Soc. London* A, **268**, 147.
BÜHLER, B., 1990, Dissertation, Universität Freiburg, Germany (in German).
BÜHLER, B., and GERBER, G., 1992, (to be published).
CHEWTER, L. A., SANDER, M., MÜLLER-DETHLEFS, K., and SCHLAG, E. W., 1987, *J. chem. Phys.*, **86**, 4737.
CHUPKA, W. A., 1992, *J. chem. Phys.*, (in press).
DE BEER, E., DE LANGE, C. A., STEPHENS, J. A., WANG, K., and MCKOY, V., 1991, *J. chem. Phys.*, **95**, 714.
DEHMER, P. M., and CHUPKA, W. A., 1976, *J. chem. Phys.*, **65**, 2243.
DIXIT, S. N., LYNCH, D. L., and MCKOY, V., 1984, *Phys. Rev.* A, **30**, 3332.
DIXIT, S. N., LYNCH, D. L., MCKOY, V., and HUO, W. M., 1985, *Phys. Rev.* A, **32**, 1267.

DIXIT, S. N., and MCKOY, V., 1985, *J. chem. Phys.*, **82,** 3546; 1986, *Chem. Phys. Lett.*, **128,** 49.
DIXON, R. N., DUXBURY, G. HORANI, M., and ROSTAS, J., 1971, *Molec. Phys.*, **22,** 977.
DUXBURY, G., JUNGEN, CH., and ROSTAS, J., 1983, *Molec. Phys.*, **48,** 719.
EDQVIST, O., LINDHOLM, E., SELIN, L. E., and ÅSBRINK, L., 1970, *Physica scripta*, **1,** 25.
EIDEN, G. C., WEINHOLD, F., and WEISSHAAR, J. C., 1991, *J. chem. Phys.*, **95,** 8665.
ELAND, J. H. D., 1984, *Photoelectron Spectroscopy*, second edition (London: Butterworth).
ERNST, W. E., SOFTLEY, T. P., and ZARE, R. N., 1988, *Phys. Rev.* A, **37,** 4172.
FANO, U., 1961, *Phys. Rev.*, **124,** 1866; 1970, *Phys. Rev.* A, **2,** 353.
FIELDING, H. H., and SOFTLEY, T. P., 1991, *Chem. Phys. Lett.*, **185,** 199; 1992, *J. Phys.* B, **25,** 4125.
FIELDING, H. H., SOFTLEY, T. P., and MERKT, F., 1991, *Chem. Phys.*, **155,** 257.
FISCHER, I., STROBEL, A., STAECKER, J., NIEDNER-SCHATTEBURG, G., MÜLLER-DETHLEFS, K., and BONDYBEY, V. E., 1992, *J. chem. Phys.*, **96,** 7171.
FROHLICH, H., GUYON, P. M., and GLASS-MAUJEAN, M., 1991, *J. chem. Phys.*, **94,** 1102.
GANTEFOR, G. F., COX, D. M., and KALDOR, A., 1990, *J. chem. Phys.*, **93,** 8395; 1991, *Ibid.*, **94,** 854.
GARTON, W. R. S., PARKINSON, W. H., and REEVES, E. M., 1962, *Proc. phys. Soc.* A, **8,** 860.
GILBERT, R. D., and CHILD, M. S., 1991, *Chem. Phys. Lett.*, **187,** 153.
GRANT, E. R., and WHITE, M. G., 1991, *Nature*, **354,** 249.
GUYON, P. M., 1991, *Laser Chem.*, **11,** 131.
GUYON, P. M., SPOHR, R., CHUPKA, W. A., and BERKOWITZ, J., 1976, *J. chem. Phys.*, **65,** 1650.
GUYON, P. M., BAER, T., NENNER, I., 1983, *J. chem. Phys.*, **78,** 3665.
GUYON, P. M., and NENNER, I., 1980, *Appl. Optics*, **19,** 4068.
HABENICHT, W., BAITER, H., MÜLLER-DETHLEFS, K., and SCHLAG, E. W., 1990b, *Physica scripta.*, **41,** 814.
HABENICHT, W., BAUMANN, R., MÜLLER-DETHLEFS, K., and SCHLAG, E. W., 1990a, *J. Electron. Spec. Rel. Phenom.*, **52,** 697.
HABENICHT, W., BAUMANN, R., MÜLLER-DETHLEFS, K., and SCHLAG, E. W., 1988, *Ber. Bunsenges. phys. Chem.*, **92,** 414; 1990b, *J. electron, Spectrosc.*, **52,** 697.
HABENICHT, W., REISER, G., and MÜLLER-DETHLEFS, K., 1991, *J. chem. Phys.*, **95,** 4809.
HABER, K. S., JIANG, Y., BRYANT, G., GRANT, E. R., and LEFEBVRE-BRION, H., 1991, *Phys. Rev.* A, **44,** R5331.
HARRINGTON, J. E., and WEISSHAAR, J. C., 1990, *J. chem. Phys.*, **93,** 854; 1992, *Ibid.*, **97,** 2809.
HEPBURN, J. W., (private communication).
HERZBERG, G., 1989, *Molecular Spectra and Molecular Structure*, Vol. 1, *Spectra of Diatomic Molecules* (Malabar, Florida: Krieger).
HERZBERG, G., and JUNGEN, CH., 1972, *J. molec. Spectrosc.*, **41,** 425.
HILLENBRAND, S., ZHU, L., and JOHNSON, P., 1991, *J. chem. Phys.*, **95,** 2237.
ITIKAWA, Y., 1978a, *Chem. Phys.*, **28,** 461; 1978b, *Ibid.*, **30,** 109.
JOHNS, J. W. C., 1974, *Molecular Spectroscopy* 2, Chem. Soc. Specialist Rep., edited by R. F. Barrow, D. A. Long and D. J. Millen (London: The Chemical Society), p. 513.
JUNGEN, CH., and RAOULT, M., 1981, *Faraday Discuss. Chem. Soc.*, **71,** 253.
KISTOPOULOS, T. N., CHICK, C. J., ZHAO, Y., and NEUMARK, D. M., 1991a, *J. chem. Phys.*, **95,** 1441; 1991b, *Ibid.*, **95,** 5479.
KONG, W., RODGERS, D., and HEPBURN, J. W., 1992, University of Waterloo, Chemical Physics Research Report.
LEAHY, D. J., REID, K. L., and ZARE, R. N., 1991, *J. chem. Phys.*, **95,** 1757.
LEE, M.-T., WANG, K., MCKOY, V., TONKYN, R. G., WIEDMANN, R. T., GRANT, E. R., and WHITE, M. G., 1992a, *J. chem. Phys.*, **96,** 7848.
LEE, M.-T., WANG, K., and MCKOY, V., 1992b, *J. chem. Phys.*, **97,** 3108.
LEFEBVRE-BRION, H., 1988, *Abstracts of International Symposium: Molecules in Physics, Chemistry and Biology*, edited by J. Maruant, Vol 2 (Dordrecht: Kluwer), p. 257; 1990a, *Chem. Phys. Lett.*, **171,** 377; 1990b, *J. chem. Phys.*, **93,** 5898; 1992, private communication.
LU, K.-T., EIDEN, G. C., and WEISSHAAR, J. C., 1992, *J. phys. Chem.*, (to be published).
LUCCHESE, R. R., RASEEV, G., and MCKOY, V., 1982, *Phys. Rev.* A, **25,** 2572.
MAHON, C. R., JANIK, G. R., and GALLAGHER, T. F., 1990, *Phys. Rev.* A, **41,** 3746.
MANK, A., DRESCHER, M., HUTH-FEHRE, T., BÖWERING, N., HEINZMANN, U., and LEFEBVRE-BRION, H., 1991, *J. chem. Phys.*, **95,** 1676.
MARANGOS, J. P., SHEN, N., MA, H., HUTCHISON, M. H. R., and CONNERADE, J. P., 1990, *J. opt. Soc. Am.* B, **7,** 1254.

MARTIN, S., CHEVALEYRE, J., VALIGNAT, S., PERROT, J. P., BROYER, M., CABAUD, B., and HOAREAU, A., 1982, *Chem. Phys. Lett.*, **87**, 235.
MERKT, F., 1992, Ph.D. Thesis, University of Cambridge (UK).
MERKT, F., FIELDING, H. H., and SOFTLEY, T. P., 1992a, *Chem. Phys. Lett.* (in press).
MERKT, F., HEPBURN, J. W., and GUYON, P. M., 1992b, (submitted).
MERKT, F., and SOFTLEY, T. P., 1990, *J. chem. Phys.*, **93**, 1540; 1992a, *Ibid.*, **96**, 4149; 1992b, *Phys. Rev.* A, 302; 1992c, unpublished results.
MORIOKA, Y., HARA, S., and NAKAMURA, M., 1980, *Phys. Rev.* A, **22**, 177.
MÜLLER-DETHLEFS, K., 1991, *J. chem. Phys.*, **95**, 4821; 1992, private communication.
MÜLLER-DETHLEFS, K., SANDER, M., and SCHLAG, E. W., 1984a, *Z. Naturf.*, **39**, 1089; 1984b, *Chem. Phys. Lett.*, **112**, 291.
MÜLLER-DETHLEFS, K., and SCHLAG, E. W., 1991, *Ann. Rev. phys. Chem.*, **42**, 109.
OKUYAMA, K., COCKETT, M. C. R., and KIMURA, K., 1992, *J. chem. Phys.*, **97**, 1649.
OZEKI, H., OKUYAMA, K., TAKAHASHI, M., and KIMURA, K., 1991a, *J. phys. Chem.*, **95**, 4308.
OZEKI, H., TAKAHASHI, M., OKUYAMA, K., and KIMURA, K., 1991b, *J. chem. Phys.*, **95**, 9401.
PEATMAN, W. B., 1976, *J. chem. Phys.*, **64**, 4368.
POLLARD, J. E., TREVOR, D. J., REUTT, J. E., LEE, Y. T., and SHIRLEY, D. A., 1982, *J. chem. Phys.*, **77**, 34.
RABALAIS, J. W., 1977, *Principles of Ultraviolet Photoelectron Spectroscopy* (New York: Wiley).
RASEEV, G., and CHEREPKOV, N. A., 1990, *Phys. Rev.* A, **42**, 3948.
RASEEV, G., GIUSTI-SUZOR, A., and LEFEBVRE-BRION, H., 1978, *J. Phys.* B, **11**, 2735.
RASEEV, G., LE ROUZO, H., and LEFEBVRE-BRION, H., 1980, *J. chem. Phys.*, **72**, 5701.
REISER, G., DOPFER, O., LINDNER, R., HENRI, G., MÜLLER-DETHLEFS, K., SCHLAG, E. W., and COLSON, S. D., 1991a, *Chem. Phys. Lett.*, **181**, 1.
REISER, G., HABENICHT, W., MÜLLER-DETHLEFS, K., and SCHLAG, E. W., 1988, *Chem. Phys. Lett.*, **152**, 119.
REISER, G., and MÜLLER-DETHLEFS, K., 1992, *J. phys. Chem.*, **96**, 9.
REISER, G., RIEGER, D., and MÜLLER-DETHLEFS, K., 1991b, *Chem. Phys. Lett.*, **183**, 239.
RIEGER, D., REISER, G., MÜLLER-DETHLEFS, K., and SCHLAG, E. W., 1992, *J. phys. Chem.*, **96**, 12.
RUDOLPH, H., DIXIT, S. N., MCKOY, V., and HUO, W. M., 1988a, *J. chem. Phys.*, **88**, 637; 1988b, *Ibid.* **88**, 1516.
SAMSON, J. A. R., and GARDNER, J. L., 1977, *J. chem. Phys.*, **67**, 755.
SANDER, M., CHEWTER, L. A., MÜLLER-DETHLEFS, K., and SCHLAG, E. W., 1987, *Phys. Rev.* A, **36**, 4543.
SICHEL, J. M., 1970, *Molec. Phys.*, **18**, 95.
SMITH, A. L., 1970a, *Phil. Trans. R. Soc. London*, A, **268**, 169; 1970b, *J. Quant. Spectrosc. Radiat. Transfer*, **10**, 1129.
SPOHR, R., GUYON, P. M., CHUPKA, W. A., and BERKOWITZ, J., 1971, *Rev. scient. Instrum.*, **42**, 1872.
STEPHENS, J. A., and MCKOY, V., 1990, *J. chem. Phys.*, **93**, 7863.
STOICHEFF, B. P., HERMAN, P. R., LAROCQUE, P. F., and LIPSON, R. H., 1985, *Laser Spectroscopy VII*, edited by T. W. Hänsch and Y. R. Shen (Berlin: Springer), p. 174.
STROBEL, A., FISCHER, I., STAECKER, J., NIEDNER-SCHATTEBURG, G., MÜLLER-DETHLEFS, K., and BONDYBEY, V. E., 1992, *J. chem. Phys.*, **97**, 2332.
TAKAHASHI, M., and KIMURA, K., 1992, *J. chem. Phys.*, **97**, 2920.
TAKAHASHI, M., OZEKI, H., and KIMURA, K., 1991, *Chem. Phys. Lett.*, **181**, 255.
TAKAZAWA, K., FUJII, M., EBATA, T., and ITO, M., 1992, *Chem. Phys. Lett.*, **189**, 592.
TONKYN, R. G., and WHITE, M. G., 1989, *Rev. scient Instrum.*, **60**, 1245; 1991, *J. chem. Phys.*, **95**, 5582.
TONKYN, R. G., WIEDMANN, R. T., GRANT, E. R., and WHITE, M. G., 1991, *J. chem. Phys.*, **95**, 7033.
TONKYN, R. G., WIEDMANN, R. T., and WHITE, M. G., 1992, *J. chem. Phys.*, **96**, 3696.
TONKYN, R. G., WINNICZEK, J. W., and WHITE, M. G., 1989, *Chem. Phys. Lett.*, **164**, 137.
TRICKL, T., CROMWELL, E. F., LEE, Y. T., and KUNG, A. H., 1989, *J. chem. Phys.*, **91**, 6006.
TURNER, D. W., BAKER, A. D., BAKER, C., and BRUNDLE, C. R., 1970, *Molecular photoelectron Spectroscopy, A Handbook of He 584 Å spectra* (New York: Interscience).
VIDAL, C. R., 1988, *Tunable lasers*, Topics in Applied Physics, edited by L. F. Mollenauer and J. C. White (Heidelberg: Springer), p. 57.
VILLAREJO, D., HERM, R. R., and INGHRAM, M. G., 1967, *J. chem. Phys.*, **46**, 4995.

VISWANATHAN, K. S., SEKRETA, E., DAVIDSON, E. R., and REILLY, J. P., 1986, *J. phys. Chem.*, **90,** 5078.

WALLENSTEIN, R., 1988, *Frontiers of Laser Spectroscopy of Gases* NATO Advanced Study Institute Series C, Vol. 234, edited by A. C. P. Alves, J. M. Brown and J. M. Hollas (Dordrecht: Kluwer), p. 53.

WALLER, I. M., KISTOPOULOS, T. N., and NEUMARK, D. M., 1990, *J. phys. Chem.*, **94,** 2240.

WANG, K., and MCKOY, V., 1991a, *J. chem. Phys.*, **95,** 7872; 1991b, **95,** 8718.

WANG, K., STEPHENS, J. A., and MCKOY, V., 1991, *J. chem. Phys.*, **95,** 6456.

WIEDMANN, R. T., GRANT, E. R., TONKYN, R. G., and WHITE, M. G., 1991, *J. chem. Phys.*, **95,** 746.

WIEDMANN, R. T., TONKYN, R. G., WHITE, M. G., WANG, K., and MCKOY, V., 1992, *J. chem. Phys.*, **97,** 768.

WIEDMANN, R. T., and WHITE, M. G., 1992, *SPIE, Optical Methods for Time- and State-resolved Chemistry*, Vol. 1638, 273.

WILKINS, R. L., and TAYLOR, H. S., 1968, *J. chem. Phys.*, **48,** 4504.

WILSON, S. H. S., MERKT, F., and SOFTLEY, T. P., 1992, (to be published).

WILSON, W. G., VISWANATHAN, K. S., SEKRETA, E., and REILLY, J. P., 1984, *J. phys. Chem.*, **88,** 672.

XIE, J., and ZARE, R. N., 1989, *Chem. Phys. Lett.*, **159,** 399; 1990, *J. chem. Phys.*, **93,** 3033; 1992, *Ibid.*, **97,** 2891.

XU, E. Y., HELM, H., and KACHRU, R., 1988, *Phys. Rev.* A, **38,** 1666.

ZHANG, X., SMITH, J. M., and KNEE, J. L., 1992, *J. chem. Phys.*, **97,** 2843.

ZHU, L., and JOHNSON, P., 1991, *J. chem. Phys.*, **94,** 5769.

ZHU, Y., GRANT, E. R., WANG, K., MCKOY, V., and LEFEBVRE-BRION, H., 1992, (in preparation).